© 2014. Published by The Company of Biologists Ltd | Development (2014) 141, 1392-1403 doi:10.1242/dev.101717

RESEARCH ARTICLE

Dynamics of Sonic hedgehog signaling in the ventral spinal cord are controlled by intrinsic changes in source cells requiring Sulfatase 1

Amir Al Oustah*, Cathy Danesin*,‡, Nagham Khouri-Farah, Marie-Amélie Farreny, Nathalie Escalas, Philippe Cochard, Bruno Glise and Cathy Soula

ABSTRACT

In the ventral spinal cord, generation of neuronal and glial cell subtypes is controlled by Sonic hedgehog (Shh). This morphogen contributes to cell diversity by regulating spatial and temporal sequences of gene expression during development. Here, we report that establishing Shh source cells is not sufficient to induce the high-threshold response required to specify sequential generation of ventral interneurons and oligodendroglial cells at the right time and place in zebrafish. Instead, we show that Shh-producing cells must repeatedly upregulate the secreted enzyme Sulfatase1 (Sulf1) at two critical time points of development to reach their full inductive capacity. We provide evidence that Sulf1 triggers Shh signaling activity to establish and, later on, modify the spatial arrangement of gene expression in ventral neural progenitors. We further present arguments in favor of Sulf1 controlling Shh temporal activity by stimulating production of active forms of Shh from its source. Our work, by pointing out the key role of Sulf1 in regulating Shh-dependent neural cell diversity, highlights a novel level of regulation, which involves temporal evolution of Shh source properties.

KEY WORDS: Shh, Sulfatase1, Floor plate, Neural cell fate, Spinal cord, Zebrafish

INTRODUCTION

In the developing ventral spinal cord, Sonic hedgehog (Shh) serves crucial roles in regulating expression of transcription factors that impose neuronal and glial subtype generation at the right time and place. Shh, produced by the notochord and medial floor plate (MFP), forms a gradient (Chamberlain et al., 2008) that initially patterns the ventral neural tube into distinct progenitor domains arrayed along the dorsoventral axis (Jessell, 2000). Nkx2.2, requiring high Shh concentrations for induction, is expressed in the ventral-most progenitors of the p3 domain, which in turn generate V3 interneurons, whereas Olig2, induced by lower Shh concentrations, is expressed dorsally, in the pMN domain, and defines the motor neuron (MN) fate (Ribes and Briscoe, 2009). Importantly, the p3 and pMN domains emerge progressively and their order of appearance corresponds with their requirement for increasing activity and duration of Shh signaling (Balaskas et al., 2012; Dessaud et al., 2010; Dessaud et al., 2007; Jeong and McMahon, 2005; Lek et al., 2010; Ribes et al., 2010). Olig2 expression is initiated before that of Nkx2.2 in the ventral neural tube. Activation of Nkx2.2 in the ventral-most progenitors further downregulates Olig2. How this Shh-dependent sequence of gene expression is regulated over time remains an open question.

After completion of MN generation, Olig2 progenitors change their fate to generate oligodendrocyte precursor cells (OPCs) (Rowitch and Kriegstein, 2010). Strikingly, this neuroglial switch is also controlled by Shh, responsible at that time for a rearrangement of the ventral patterning, resulting in generation of the p* domain. This domain forms following dorsal expansion of Nkx2.2 expression in Olig2 progenitors in response to a rise in Shh signaling (Agius et al., 2004; Danesin et al., 2006; Fu et al., 2002; Touahri et al., 2012; Zhou et al., 2001). At this stage, Nkx2.2 no longer represses Olig2 and their co-expression drives p* progenitors to the OPC fate. We identified the secreted enzyme Sulfatase1 (Sulf1) as a major player in triggering this cell fate change in amniotes (Touahri et al., 2012). By modulating the sulfation state of heparan sulphate proteoglycans (HSPGs) at the cell surface, Sulf1 regulates interaction of HSPGs with morphogen factors (Ai et al., 2003; Dhoot et al., 2001; Freeman et al., 2008; Lamanna et al., 2007; Meyers et al., 2013; Viviano et al., 2004; Wang et al., 2004). In *Drosophila*, Sulf1 has opposing functions, enhancing Hh release from its source and reducing Hh signaling activity in the responding cells (Wojcinski et al., 2011). In vertebrate spinal cord, Sulf1 only behaves as a positive modulator of Shh signaling (Danesin et al., 2006; Touahri et al., 2012). Strikingly, the expression of Sulf1 is highly dynamic in this tissue. Its function in triggering the MN/OPC fate switch is related to its upregulation in Nkx2.2 progenitors (Braquart-Varnier et al., 2004; Danesin et al., 2006; Touahri et al., 2012), suggesting that Sulf1, by lowering the Shh-HSPG interaction at the surface of p3 progenitors, helps to provide higher doses of Shh, free to travel dorsally, to Olig2 progenitors. However, the mechanism by which Sulf1 non-cell autonomously activates Shh signaling has yet to be elucidated.

Before patterning rearrangement, Sulf1 is expressed in the ventral neural tube (Braquart-Varnier et al., 2004; Danesin et al., 2006; Gorsi et al., 2010; Meyers et al., 2013; Touahri et al., 2012), opening the possibility that it could also influence Shh signaling at stages of patterning establishment. We report that, in addition to its function in stimulating OPC induction, Sulf1 activity is crucial for generation of ventral neuronal subtypes in zebrafish. We show that Sulf1 acts as a temporal amplifier to trigger high-threshold response to Shh and thereby to successively foster ventral patterning establishment and rearrangement. Of importance, we show that Sulf1 regulates the dynamics of Shh signaling by changing the inductive properties of Shh source cells at these two critical time points, and provide arguments in favor of Sulf1 stimulating provision of a biologically active form of Shh.

University of Toulouse, Center for Developmental Biology, UMR 5547 CNRS, 118 Route de Narbonne, 31062 Toulouse, France.
*These authors contributed equally to this work

‡Author for correspondence (cathy.danesin@univ-tlse3.fr)

Received 30 July 2013; Accepted 6 January 2014

Development (2014) doi:10.1242/dev.101717

RESULTS

Sulf1 depletion impairs generation of OPCs and V3 interneurons in zebrafish

To address the role of Sulf1, we used a morpholino oligonucleotide (MO) knockdown approach and a *sulf1* mutant background in zebrafish. Two MOs blocking either *sulf1* translation (*sulf1*MO^{ATG}) or splicing (*sulf1*MO^{splice}) were designed. RT-PCR performed on RNA harvested from *sulf1*MO^{splice}-injected embryos confirmed the efficacy of *sulf1* knockdown at least until 72 hours post-fertilization (hpf; supplementary material Fig. S1). As similar results were obtained using either MO, used in parallel in all experiments, they are referred to as *sulf1*MO. Molecular analysis of *sulf1*^{sa199} showed that the point mutation mapping the *sulf1* locus in this line resulted in a premature stop codon included in the hydrophilic domain of the protein, required for Sulf1-HSPG interaction (Ai et al., 2006; Dhoot et al., 2001).

We first investigated whether Sulf1 is required for OPC generation in zebrafish. *Sulf1*MO was injected into *Tg(olig2:EGFP)* embryos in which GFP-positive (GFP+) OPCs can be identified by their morphology and position (Shin et al., 2003). At 48 hpf, the number of OPCs was significantly reduced in *sulf1*MO-injected embryos compared with ctrlMO-injected embryos (Fig. 1A-C). Similar results were obtained at 72 hpf in *Tg(nkx2.2a:mEGFP;olig2:dsRed2)* larvae in which OPCs were marked by GFP and dsRed co-expression (Fig. 1D-F). We analyzed expression of *mbpa*, a hallmark of oligodendroglial differentiation (Brösamle and Halpern, 2002), in *sulf1*MO-injected and *sulf1*$^{sa199-/-}$ larvae. At 72 hpf, *sulf1* morphant and mutant larvae had fewer *mbpa*+ cells than wild-type larvae or *sulf1* mismatch-MO- and ctrlMO-injected larvae (Fig. 1G-M; data not shown). Of note, reduction in the number of *mbpa*+ cells was less pronounced in *sulf1*$^{sa199+/-}$ than in *sulf1*$^{sa199-/-}$ larvae (Fig. 1K-M), indicating a gene dosage effect of *sulf1*, as previously reported in mouse (Touahri et al., 2012). Thus, similar to in mouse, Sulf1 activity is required for the proper generation of OPCs in zebrafish.

We next addressed the role of Sulf1 on neuronal generation. We first used *tal2* expressed in Kolmer-Agduhr (KA) interneurons originating from pMN and p3 progenitors (Huang et al., 2012; Schäfer et al., 2007; Yang et al., 2010). At 24 hpf, *tal2*+ neurons were severely reduced in number (Fig. 2A-H), in both *sulf1*MO-injected and *sulf1*$^{sa199-/-}$ embryos compared with embryos injected with *sulf1* mismatch MO or ctrlMO and wild-type embryos. Again, *sulf1*$^{sa199+/-}$ embryos displayed a less severe phenotype than *sulf1*$^{sa199-/-}$ siblings (Fig. 2E,F,H). We further analyzed *islet2a*, expressed in primary MNs generated early (13 hpf) from the ventral-most neural progenitors (Appel et al., 1995; Schäfer et al., 2007), and *sim1*, detected later in V3 interneurons originating from progenitors expressing *nkx2.2a* (p3 domain) (Schäfer et al., 2007). We found that although generation of *islet2a*+ primary MNs was unaffected, the number of *sim1*+ V3 interneurons was significantly reduced in *sulf1*MO-injected embryos (Fig. 2I-N), indicating that *sulf1* depletion preferentially impairs generation of V3 interneurons.

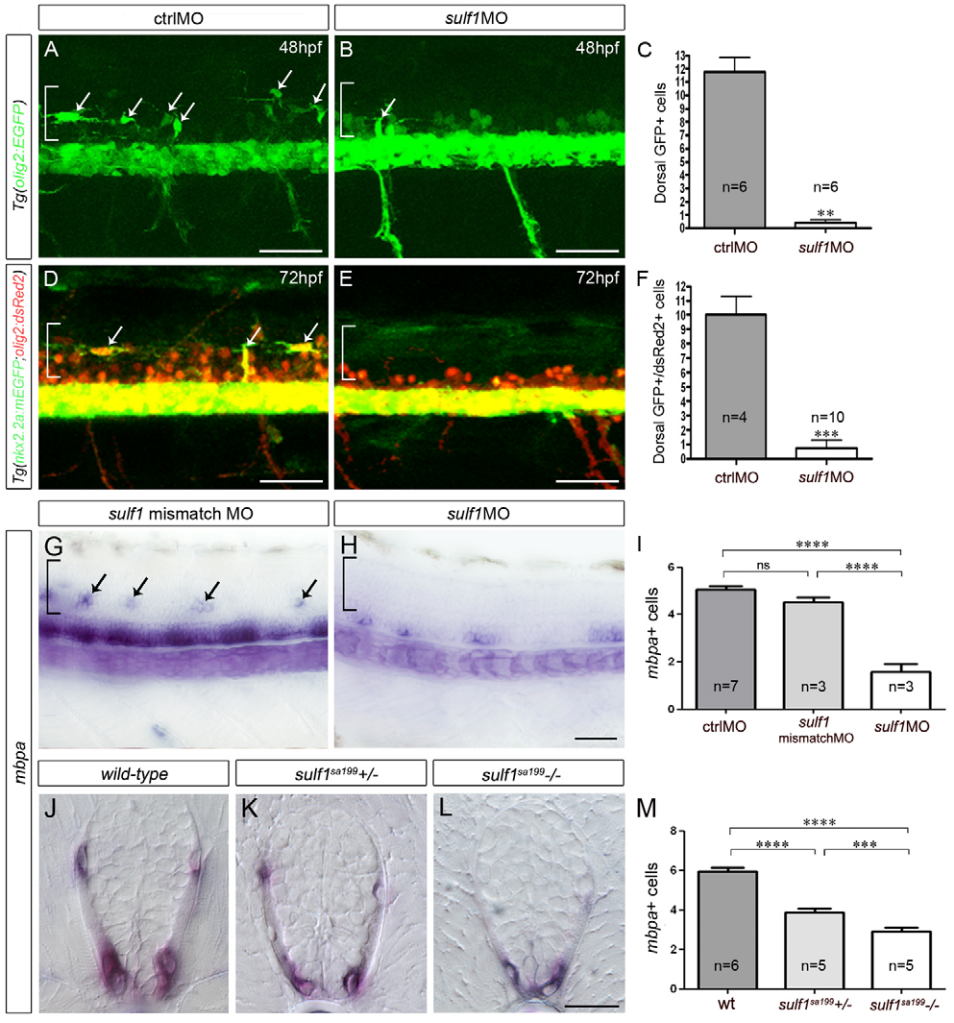

Fig. 1. *Sulf1* depletion impairs OPC development in zebrafish. A-H show side views of whole embryos at the level of the trunk spinal cord; anterior to the left and dorsal to the top. J-L show transverse spinal cord sections, dorsal to the top. (A-C) Detection (A,B) and quantification (C) of dorsal OPCs (arrows) at 48 hpf in Tg(*olig2*:GFP) embryos injected with ctrlMO (A) and *sulf1*MO (B). (D-F) Detection (D,E) and quantification (F) of dorsal OPCs (arrows) at 72 hpf in *Tg(nkx2.2a:mEGFP;olig2:dsRed2)* larvae injected with ctrlMO (D) and *sulf1*MO (E). (G,H,J-L) Expression of *mbpa* at 72 hpf in larvae injected with *sulf1* mismatch MO (G) and *sulf1*MO (H) and in wild-type (J), *sulf1*$^{sa199+/-}$ (K) and *sulf1*$^{sa199-/-}$ (L) larvae. (I,M) Quantification of *mbpa*+ cells in transverse sections of morphants (I) and *sulf1*$^{sa199+/-}$ incross progeny (M). Results are presented as mean number of cells ± s.e.m. (**P<0.01, ***P<0.001, ****P<0.0001; ns, non-significant). Brackets indicate position of the dorsal spinal cord. Scale bars: 100 µm (A-H), 50 µm (J-L).

Development (2014) doi:10.1242/dev.101717

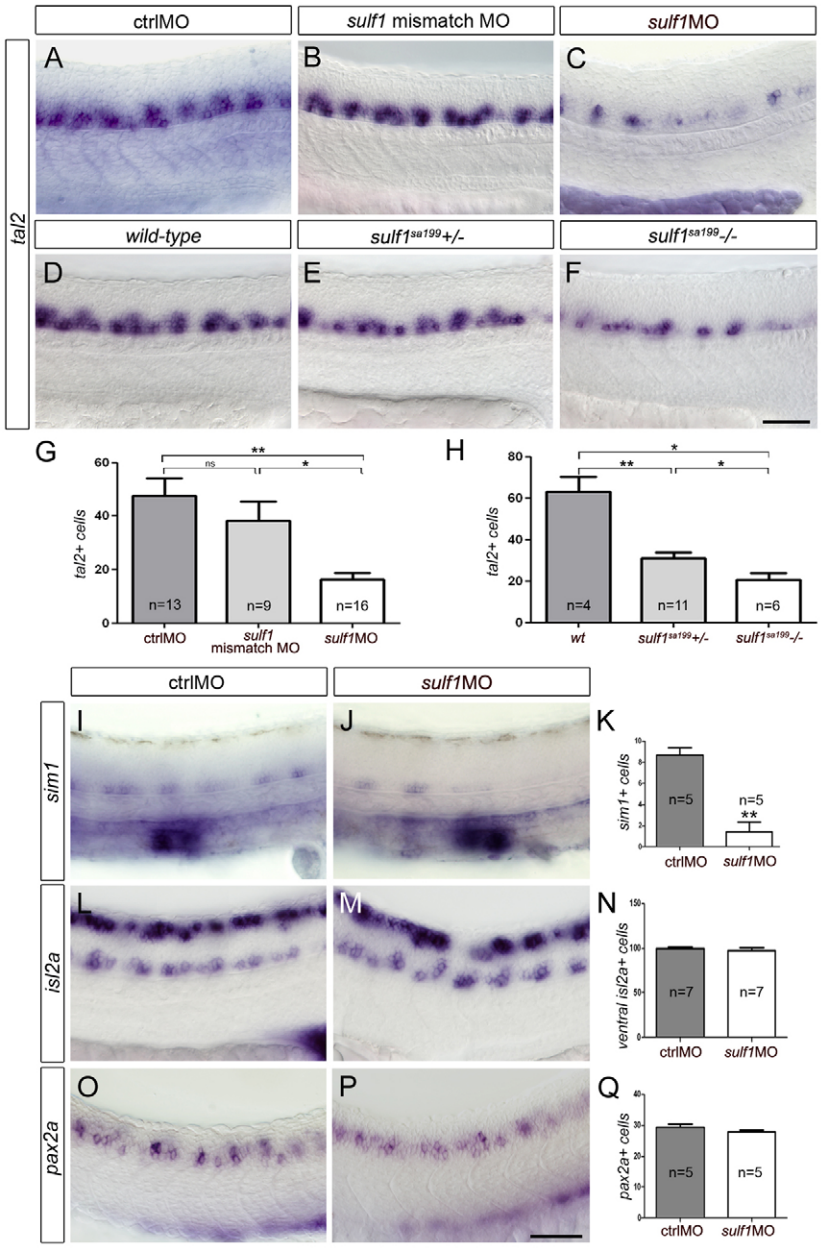

Fig. 2. *Sulf1* depletion impairs generation of ventral neuronal subtypes. Side views of whole embryos at the level of the trunk spinal cord, anterior to the left and dorsal to the top. (A-H) Detection (A-F) and quantification (G,H) of *tal2*-expressing neurons at 24 hpf in embryos injected with ctrlMO (A), *sulf1* mismatch MO (B) and *sulf1*MO (C) and in wild-type (D), *sulf1*$^{sa199+/-}$ (E) and *sulf1*$^{sa199-/-}$ (F) embryos. (I-Q) Detection and cell counts of *sim1*+ (I-K), *islet2a*+ MNs (L-N) and *pax2a*+ dorsal neurons (O-Q) in embryos injected with ctrlMO (I,L,O) and *sulf1*MO (J,M,P). Results are presented as mean number of cells ± s.e.m. (**P*<0.05, ***P*<0.01). Scale bars: 100 µm.

Finally, injection of *sulf1*MO had no effect on generation of *pax2a*+ dorsal neurons (Fig. 2O-Q), position of which but not production of which depends on Shh (England et al., 2011).

Altogether, our data highlight the function of Sulf1 in triggering OPC production in zebrafish and reveal a novel role for the enzyme in controlling the Shh-dependent generation of ventral neuronal subtypes.

Expression of *sulf1* is restricted to Shh-producing cells of the developing spinal cord

To gain insights into Sulf1 function, we compared expression of *sulf1* and *shh* in the embryonic spinal cord. As previously reported (Concordet et al., 1996; Krauss et al., 1993), *shh* was expressed in MFP cells as soon as 12 hpf (Fig. 3E). By contrast, *sulf1* expression was not detected at this early stage (Fig. 3A). It became apparent only from 14 hpf in Shh-expressing MFP cells (Fig. 3B,F) and its expression was restricted to MFP until 24 hpf (Fig. 3C,G). Therefore, at stages of ongoing neuronal production (Myers et al., 1986), *sulf1* is upregulated in cells that already express *shh* and remains restricted to Shh source cells.

Expression of *shh* is known to expand dorsally as development proceeds to form a novel ligand source, named the lateral floor plate (LFP) (Charrier et al., 2002; Park et al., 2004). In zebrafish, LFP forms at 36 hpf, i.e. at the onset of OPC generation. At this stage, we found that *sulf1* expression also expanded dorsally, into LFP cells (Fig. 3D,H). Therefore, *sulf1* is expressed in Shh source cells at the same stages of OPC generation in zebrafish. This prompted us to examine whether, in chicken, *sulf1*-expressing cells are also Shh source cells as they stimulate OPC induction (Touahri et al., 2012). We found that, in chicken, cells of the p3 domain express *shh* as they upregulate *sulf1* (supplementary material Fig. S2A-C). Importantly, as observed in the zebrafish MFP (Fig. 3), Shh expression in p3 cells precedes that of Sulf1 (supplementary material Fig. S2D-F).

Together, these data reveal that Sulf1 is specifically expressed in Shh source cells both in zebrafish and chicken, and that its

Development (2014) doi:10.1242/dev.101717

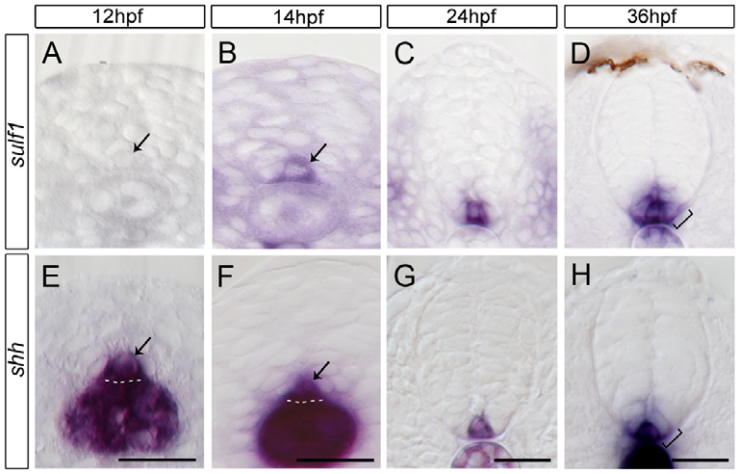

Fig. 3. *Sulf1* is specifically upregulated in *shh*-expressing MFP and LFP cells at the two critical time points of neuronal and OPC generation. Transverse sections through trunk spinal cord are shown; dorsal to the top in all panels. (A-H) Temporal expression of *sulf1* (A-D) and *shh* (E-H). At 12 hpf, MFP (arrows) expresses *shh* (E) but not *sulf1* (A). From 14 hpf, both transcripts are detected in MFP cells (arrows, B,F). At 36 hpf, *sulf1* (D) and *shh* (H) are expressed in MFP and LFP (brackets). Dashed lines outline the ventral border of the neural tube. Scale bars: 20 µm.

expression is reiteratively initiated in MFP and LFP cells after *shh* upregulation. In the following sections, the ventral-most progenitor domain is referred to as the p3 domain prior to *shh* upregulation and as the LFP once it gains expression of *shh*.

Sulf1 is required to activate high-threshold response to Shh at the right time and place

Our data so far has identified that Sulf1 is involved in controlling generation of V3 interneurons. This prompted us to examine its function in establishment of the p3 domain. Although spatial patterning of the neural tube is known to be conserved in zebrafish (Guner and Karlstrom, 2007), the temporality of its establishment remains to be explored. We examined the expression time course of *olig2* and *nkx2.2*, named *nkx2.2a* in zebrafish (Kucenas et al., 2008a), known to be differentially sensitive to Shh signaling levels in zebrafish (Barth and Wilson, 1995; Guner and Karlstrom, 2007; Park et al., 2002). As previously reported (Park et al., 2002), *olig2* was expressed from 12 hpf (data not shown). At 14 hpf, the *olig2*+ domain was in a very ventral location, abutting the MFP (Fig. 4A). *nkx2.2a* expression was not detected at this stage (Fig. 4D) but became apparent from 16 hpf in cells abutting the MFP as they had

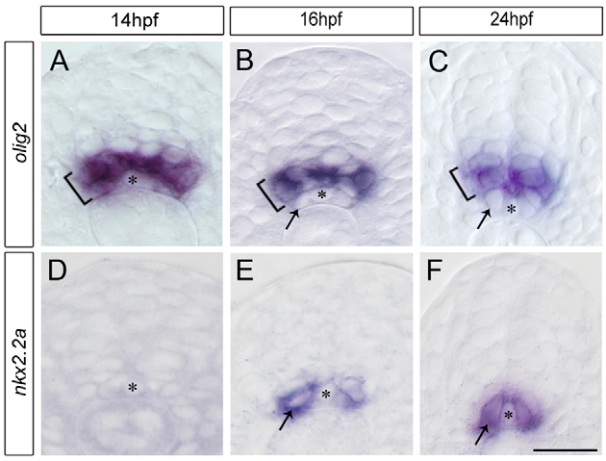

Fig. 4. Sequential expression of *olig2* and *nkx2.2a* in the zebrafish neural tube. (A-F) Expression of *olig2* (A-C, brackets) and *nkx2.2a* (D-F) on transverse sections of 14 hpf (A,D), 16 hpf (B,E) and 24 hpf (C,F) embryos. Expression of *nkx2.2a* is detected from 16 hpf (E,F) in cells (arrows) abutting the MFP, which at the same time downregulate *olig2* (BC). Asterisks in all panels mark the MFP. Scale bar: 20 µm.

downregulated *olig2* (Fig. 4B,E). At 24 hpf, *nkx2.2a* and *olig2* expression defined two adjacent non-overlapping domains, reflecting establishment of the ventral patterning (Fig. 4C,F). Therefore, in zebrafish, progressive formation of the p3 and pMN domains occurs between 14 and 16 hpf. Note that this time period immediately follows *sulf1* activation in MFP cells (Fig. 3B).

We next assessed the role of *sulf1* on the sequential activation of *olig2* and *nkx2.2a*. We found that *olig2* expression persisted at 16 hpf in *sulf1*MO-injected embryos (Fig. 5A,D). However, the *olig2*+ domain did not shift dorsally and this gene continued to be expressed in progenitors abutting the MFP (Fig. 5D). In agreement, *nkx2.2a* failed to be upregulated in 16 hpf *sulf1* morphants (Fig. 5B,E). Therefore, *sulf1* depletion interferes with Shh-mediated neural tube patterning by preventing *nkx2.2a* induction at the proper time. Furthermore, *foxa2* expression, a hallmark of MFP and p3 cells at 16 hpf (Schäfer et al., 2007), was restricted to MFP cells in *sulf1* morphants (Fig. 5C,F), confirming deficient generation of the p3 domain and, of importance, showing that Sulf1 is dispensable for proper formation and maintenance of MFP cells. Moreover, as *foxa2* expression in p3 cells but not in MFP cells depends on Shh (Odenthal et al., 2000; Schäfer et al., 2007), these results argue in favor of *sulf1* acting by stimulating Shh signaling.

To determine whether the phenotype of 16 hpf *sulf1* morphants reflected only a slight delay in p3 induction, we analyzed *sulf1*-depleted embryos at 24 hpf. We found that *sulf1*MO-injected embryos maintained *olig2* expression in MFP adjacent cells (Fig. 5G,J) and still failed to upregulate *nkx2.2a* (Fig. 5H,K,L; data not shown). To confirm the specific involvement of *sulf1*, we co-injected *sulf1*MO^{splice} and *sulf1* mRNA and found a significant rescue (51%, n=65) of *nkx2.2a* expression at 24 hpf (Fig. 5I). *nkx2.2a* also failed to be expressed at 24 hpf in *sulf1*$^{sa199-/-}$ embryos (Fig. 5M,N). Furthermore, 24 hpf *sulf1*MO-injected embryos also failed to upregulate *nkx2.9*, specifically expressed in p3 cells (Guner and Karlstrom, 2007; Xu et al., 2006), whereas *pax7a* expression in dorsal progenitors and *arx*, expressed in MFP cells (Norton et al., 2005), were unaffected (supplementary material Fig. S3). This further supports that *sulf1* is specifically required for Shh-dependent neural patterning. Together, these data, showing that Sulf1 is required for induction of high-threshold Shh responsive genes, support the view that the enzyme controls the establishment of the ventral patterning by sustaining and/or enhancing Shh signaling activity.

We previously reported that *sulf1*-deficient mouse embryos express Nkx2.2 and the positioning of the pMN domain at the onset

Development (2014) doi:10.1242/dev.101717

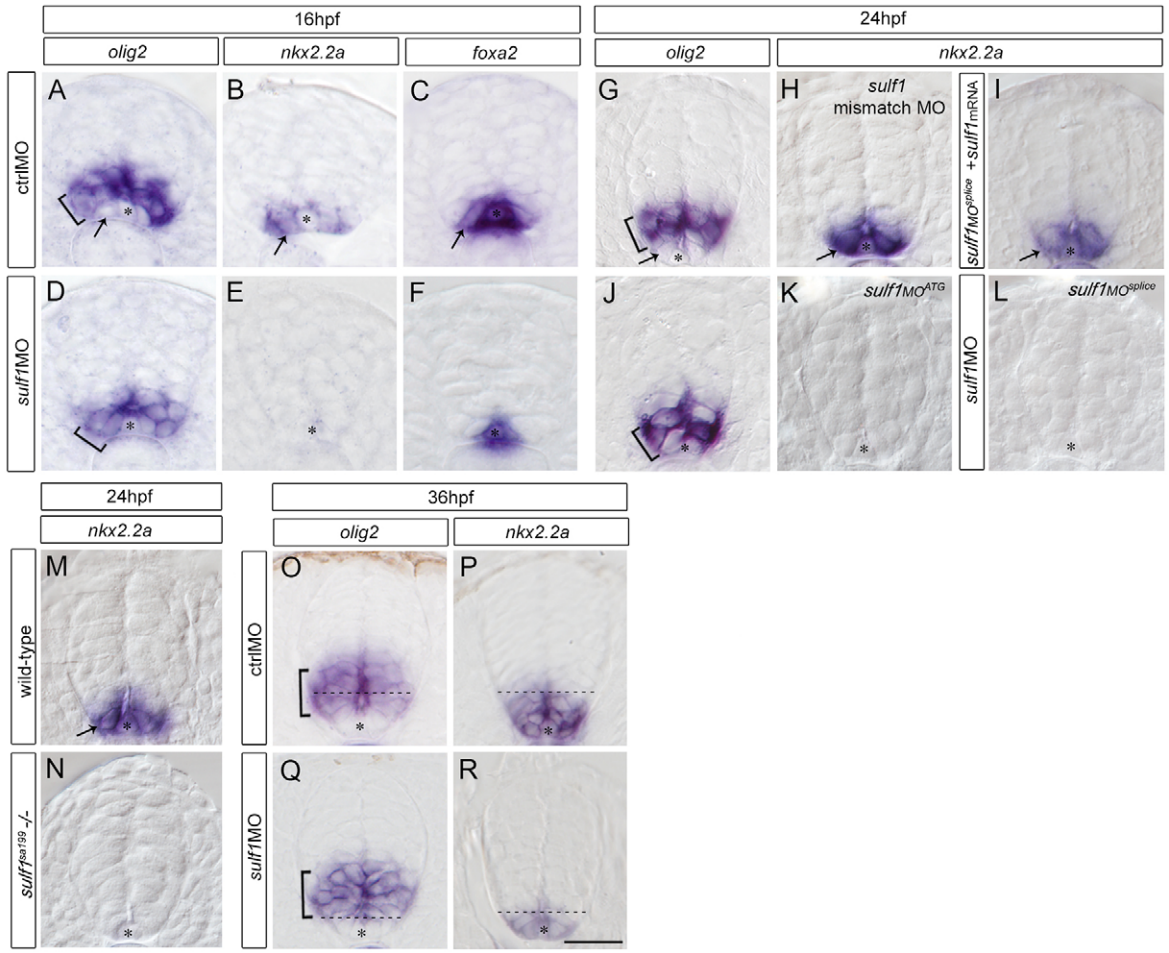

Fig. 5. *Sulf1* is required for correct temporal establishment and rearrangement of ventral neural patterning. (A-F) Expression of o*lig2* (A,D), *nkx2.2a* (B,E) and *foxa2* (C,F) in transverse sections at 16 hpf in ctrlMO-injected (A-C) and *sulf1*MO-injected (D-F) embryos. Injection of ctrlMO does not affect expression of *olig2* (A), *nkx2.2a* (B) and *foxa2* (C), but injection of *sulf1*MO prevents upregulation of *nkx2.2a* (E) and *foxa2* (F) as well as the dorsal shift of the *olig2*+ domain (D). (G-L) Expression of o*lig2* (G,J) and *nkx2.2a* (H,I,K,L) at 24 hpf in embryos injected with ctrlMO (G), mismatch MO (MisMO, H), *sulf1*MO^{ATG} (K), *sulf1*MO^{splice} (L) and co-injected with *sulf1*MO^{splice} and *sulf1* mRNA (I). (M,N) Expression of *nkx2.2a* at 24 hpf in wild-type (M) and *sulf1*$^{sa199-/-}$ (N) embryos. (O-R) Expression of o*lig2* (O,Q) and *nkx2.2a* (P,R) at 36 hpf in embryos injected with ctrlMO (O,P) and *sulf1*MO (Q,R). Brackets indicate position of the *olig2*+ domain, arrows point to *nkx2.2a*+ cells and stars mark the MFP in all panels. Dashed lines in O-R indicate dorsal boundary of the *nkx2.2a*+ domain. Scale bar: 20 µm.

of OPC generation is normal (Touahri et al., 2012), suggesting either species differences between mouse and zebrafish or a possible restoration of *nkx2.2* expression over time. Arguing in favor of a conserved function for *sulf1* in controlling patterning establishment, we found that *sulf1* is required also in mice for proper formation of the p3 domain as assessed by reduction in the dorsal expansion of the Nkx2.2+ domain at E9.5 in *sulf1*$^{-/-}$ mutant embryos compared with wild-type siblings (supplementary material Fig. S4). We next monitored *nkx2.2a* expression at 36 hpf in zebrafish morphants to determine whether its expression had also been restored at initiation of OPC generation. In control zebrafish embryos, the *nkx2.2a*+ domain expanded dorsally, within the *olig2*+ domain, establishing conservation of patterning rearrangement and formation of the p* domain (Fig. 5O,P; ctrlMO, *n*=4). At this stage, we found that *sulf1* depletion did not alter positioning of the *olig2*+ domain (Fig. 5Q). Consistently, *nkx2.2a* was expressed in ventrally located cells, indicating that formation of the p3 domain, although delayed (24-36 hpf instead of 16 hpf), had been restored. However, the *nkx2.2a*+ domain was markedly reduced in size and did not overlap the *olig2*+ domain (Fig. 5Q,R), indicating that *sulf1* function is also required for formation of the p* domain in zebrafish. However, restoration of the p3 domain at 36 hpf in morphants indicates that Sulf1 function in patterning establishment has been compensated over time.

Together, these data, showing that Sulf1 is required during development for establishment of the ventral patterning at the correct time and, later, its rearrangement, argue in favor of Sulf1 acting as a temporal amplifier to trigger expression of high-threshold Shh responsive genes at two critical time periods of spinal cord development.

Sulf1 depletion impairs Shh signaling levels without disrupting *shh* expression

We further investigated whether *sulf1* controls Shh signaling by regulating *shh* expression in ligand source cells. We found that, at 16, 24 or 36 hpf, ctrlMO- and *sulf1*MO-injected embryos expressed similar levels of *shh* mRNA in the MFP and LFP (Fig. 6A-F). Similar results were obtained using the *Tg(shh:EGFP)* line in which GFP expression is driven by *shh* regulatory regions (Shkumatava et al., 2004) (Fig. 6G-J). At all stages, expression of *patched2* (*ptc2*),

Development (2014) doi:10.1242/dev.101717

used as a reporter of Shh signaling activity (Concordet et al., 1996), was severely decreased in both *sulf1*MO-injected and *sulf1*$^{199-/-}$ embryos (supplementary material Fig. S5), confirming that *sulf1* depletion prevents full activation of Shh signal transduction. Together, these results support a role of Sulf1 in stimulating Shh signaling activity without regulating *shh* expression, at least at a transcriptional level.

Partial inactivation of Shh signal transduction is sufficient to prevent formation of the p3 and p* domains

We next examined how upregulation of *sulf1* in Shh-producing cells contributes to activate Shh signaling. An attractive possibility was that Sulf1 expression in Shh source cells stimulates the release of Shh, thereby promoting the delivery of higher amount of the morphogen. We reasoned that, if bursts of Shh are indeed required for formation of the p3 and p* domains, partial inhibition of Shh signal transduction in target cells, by mimicking reduced levels of Shh, should prevent *nkx2.2a* upregulation, as observed in *sulf1*-depleted embryos. To test this, we used cyclopamine, a potent inhibitor of Shh signaling, which acts by antagonizing the Shh co-receptor Smoothened (Smo) (Cooper et al., 1998; Incardona et al., 1998). As cyclopamine used at 100 µM totally abolishes *olig2* and *nkx2.2a* expression (Park et al., 2004; Stamataki et al., 2005), we incubated embryos in 5 µM cyclopamine from 14 hpf, when *sulf1* is upregulated in MFP cells (Fig. 3). At 24 hpf, embryos expressed neither *olig2* nor *nkx.2.2a* (Fig. 7A-D), indicating that 5 µM cyclopamine inhibits Shh signaling below levels required to maintain *olig2* and induce *nkx2.2a*. We then used cyclopamine at 1 µM and observed that embryos still expressed *olig2* in cells abutting the MFP (Fig. 7E,J) but failed to upregulate *nkx2.2a* (Fig. 7F,K). Confirming lack of p3 cells at this dose, *foxa2* expression was restricted to MFP cells (Fig. 7I,L). As ongoing Shh signaling is required to maintain *olig2* expression (Park et al., 2004), these results indicate that 1 µM cyclopamine does not totally abolish Shh signaling. Therefore, partial inactivation of Shh signal transduction between 14 and 24 hpf is sufficient to prevent *nkx2.2a* upregulation in the prospective p3 domain, mimicking *sulf1* depletion.

We next monitored the effects of cyclopamine when added at 30 hpf. In agreement with a high level of Shh signaling activity being required to induce OPCs in chicken (Danesin et al., 2006), incubation of *Tg(olig2:*EGFP*)* larvae in either 5 or 1 µM cyclopamine impaired OPC generation at 72 hpf (Fig. 7M-O). As observed at earlier stages, 5 µM but not 1 µM cyclopamine treatment abolished *olig2* expression at 48 hpf (Fig. 7P,R,T). Instead, and in agreement with Shh being required for *nkx2.2* upregulation but not its maintenance (Agius et al., 2004; Allen et al., 2011), we found that *nkx2.2a* was expressed at both doses of cyclopamine (Fig. 7S,U). However, 1 µM cyclopamine was sufficient to prevent dorsal expansion of the *nkx2.2a*+ domain (Fig. 7Q,U). Therefore, partial inhibition of Shh signal transduction from 30 hpf is sufficient to prevent formation of the p* domain at the correct time, while leaving the p3 and pMN domains unaffected, again mimicking *sulf1* depletion.

Together, these data reveal that higher threshold activation of the Shh co-receptor Smo is required at the two critical time periods of patterning, i.e. establishment (14-24 hpf) and rearrangement (30-48 hpf), supporting the view that higher amount of Shh ligand must be provided to ventral cells for formation of the p3 and p* domains at the correct time. As *sulf1* depletion and partial blockade of Smo activity resulted in similar phenotypes, we conclude that expression of Sulf1, first in MFP cells and later in LFP cells, results in provision of higher amount of Shh to ventral target cells.

Sulf1 regulates production of a biologically active form of Shh from its source cells

To investigate Sulf1 function further, we turned to cultures of chicken spinal cord explants, in which it is possible to see Shh directly in living tissue (Danesin et al., 2006). In these experiments, we used the 5E1 monoclonal antibody that recognizes the biologically active form of Shh (Ericson et al., 1996). This conformation-dependent antibody indeed specifically binds to the Shh zinc coordination site, also identified as the binding site for Shh receptors (Bishop et al., 2009; Bosanac et al., 2009; Maun et al., 2010). We first examined Shh distribution over the culture period, corresponding to the time window of active patterning rearrangement (Fig. 8A,B). A few hours after plating, equivalent to 4.5 days of development (E4.5) *in vivo*, 5E1 staining identified immunoreactive punctae concentrated apically at the surface of MFP cells expressing *shh* (Fig. 8C,F). Strikingly, the 5E1 immunoreactive form of Shh was not detected in the apical compartment of Nkx2.2+ cells, which are part of the receiving field at this stage (Fig. 8C). After 2 days in culture, equivalent to E6.5 *in vivo*, the 5E1 immunoreactive punctae covered a much broader domain, encompassing the MFP and LFP, the latter being marked by Nkx2.2 expression (Fig. 8D,G). Again, we did not detect 5E1

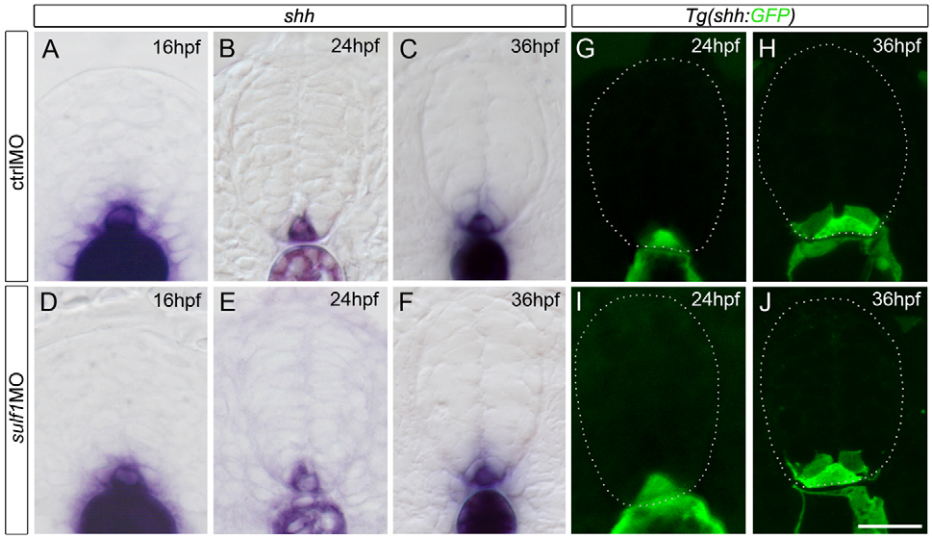

Fig. 6. Expression of s*hh* is unaffected in *sulf1*-depleted embryos. (A-F) Expression of *shh* in ctrlMO-injected (A-C) and *sulf1*MO-injected (D-F) embryos at 16 hpf (A,D), 24 hpf (B,E) and 36 hpf (C,F). (G-J) Detection of GFP at 24 hpf (G,I) and 36 hpf (H,J) in ctrlMO-injected (G,H) and *sulf1*MO-injected (I,J) *Tg(shh:GFP)* embryos. Dashed lines outline the spinal cord. Scale bar: 20 µm.

Development (2014) doi:10.1242/dev.101717

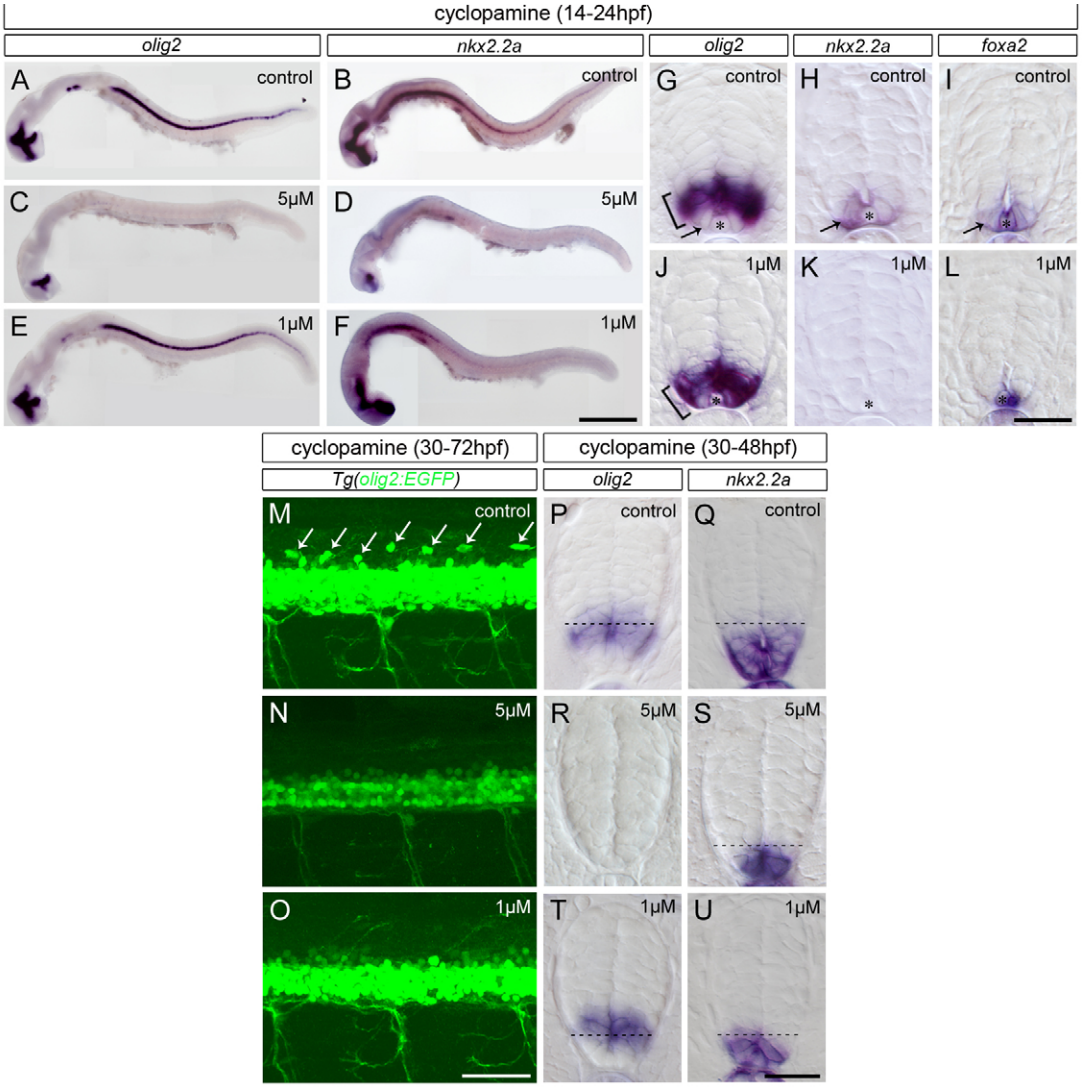

Fig. 7. Partial inhibition of Hh signal transduction prior to each step of patterning progression is sufficient to prevent the correct temporal formation of the p3 and p* domains. Panels A-F and M-O show side views of whole embryos; all other panels show spinal cord transverse sections. (A-L) Expression of *olig2* (A,C,E; brackets in G,J), *nkx2.2a* (B,D,F; arrow in H,K) and *foxa2* (I,L) at 24 hpf in embryos incubated from 14 hpf in control solution (A,B,G-I) or in cyclopamine at 5 μM (C,D) or 1 μM (E,F,J-L). Note that 1 μM cyclopamine-treated embryos express *olig2* (J) but not *nkx2.2a* (K) and *foxa2* (L) in cells abutting the MFP (asterisks). (M-O) Detection of GFP at 72 hpf in *Tg(olig2:EGFP)* larvae incubated from 30 hpf in control solution (M) or in cyclopamine at 5 μM (N) and 1 μM (O). (P-U) Expression of *olig2* (P,R,T) and *nkx2.2a* (Q,S,U) at 48 hpf in embryos incubated from 30 hpf in control solution (P,Q) or in cyclopamine at 5 μM (R,S) or 1 μM (T,U). Dashed lines indicate dorsal boundary of the *nkx2.2a*+ domain. Scale bars: 200 μm in A-F; 50 μm in M-O; 20 μm in G-L,P-U.

immunoreactivity at the surface of Shh-receiving cells, as assessed by lack of signal at the apical surface of Olig2+ progenitors (Fig. 8D). Lack of 5E1 signal in the receiving field might reflect either low amounts of Shh, below the limit of detection, or, as the 5E1 epitope is masked by Shh binding to its receptors (Bosanac et al., 2009; Maun et al., 2010), inability of the antibody to access its epitope. In support of the latter interpretation, detection of 5E1 immunoreactivity at the surface of LFP cells is temporally correlated with downregulation of the receptor *ptc* in these cells (Touahri et al., 2012). In any case, these experiments indicate that 5E1 antibody is an invaluable tool to specifically mark Shh at the apical surface of ligand source cells. We therefore used this experimental paradigm to investigate the possibility that Sulf1 controls Shh production at the source level. To test this, we impaired Sulf1 function using a blocking antibody (αSulf1) or electroporation of a *sulf1*RNAi expression vector (Touahri et al., 2012). We found that 5E1 immunoreactivity was still apparent at the apical surface of MFP and LFP cells in explants treated for 2 days with αSulf1 (Fig. 8E). However, both the density of immunoreactive punctae and intensity of the fluorescent staining at MFP and LFP cell surfaces was markedly reduced (Fig. 8I). Confirming that *shh* transcriptional regulation does not depend on Sulf1, expression of *shh* mRNA was unaffected in these explants (Fig. 8H). Similarly, expression of *sulf1*RNAi significantly reduced the 5E1 signal at the apical surface of electroporated cells compared with non-electroporated cells (Fig. 8K-L), whereas electroporation of a control RNAi vector (gfpRNAi) did not affect this signal (Fig. 8J,J′,L).

Together, these results, showing that Sulf1 inactivation reduces levels of the 5E1 signal at MFP and LFP cell surfaces, supporting the view that Sulf1 controls production of Shh at the source level. Reduction in the 5E1 signal after Sulf1 inactivation might reflect either a decrease in the total amount of Shh through stimulation of Shh release or a reduction in the 5E1 epitope accessibility because of defective processing of Shh. According to the first interpretation,

Development (2014) doi:10.1242/dev.101717

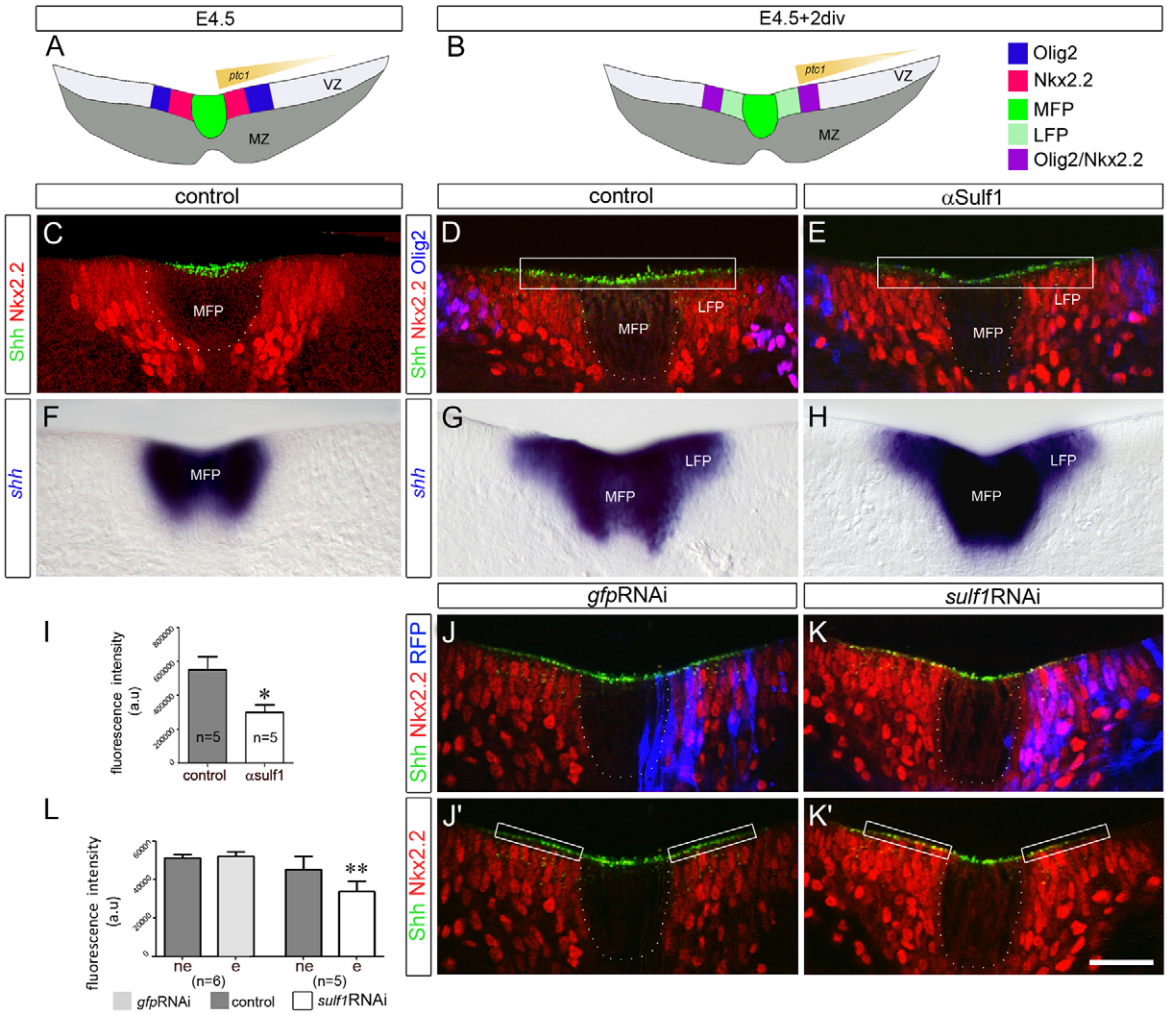

Fig. 8. *Sulf1* inactivation reduces production of 5E1 immunoreactive forms of Shh at the apical surface of morphogen source cells. (A,B) Schematic of MFP, LFP and neural domain organization on transverse sections of chicken spinal cord explants [from Touahri et al. (Touahri et al., 2012) and supplementary material Fig. S2]. At E4.5, coexpression of *shh* and *sulf1* is restricted to the MFP (green, A) and expands to the LFP (light green) after 2 days *in vitro* (E4.5+2div; B). Expression of Nkx2.2 initially defines the p3 domain (red) included in the Shh-responsive field (A). Following LFP formation in the former p3 domain, Olig2 progenitors upregulate Nkx2.2 in response to Shh, leading to formation of the p* domain (purple). (C-E) Immunodetection of Shh (green), Nkx2.2 (red) and Olig2 (blue in D,E) 3 hours (C) and 2 days (D,E) after plating. The 5E1 signal is detected at the apical surface of MFP cells at E4.5 (C) and of MFP/LFP cells at E4.5+2div (D) but not at the surface of Shh-responding cells, i.e. Nkx2.2+ cells at E4.5 (red, C) and Olig2+ cells at E4.5+2div (blue, D). Only a weak 5E1 signal is detected in αSulf1-treated explants (E). (I) Fluorescence intensity of the 5E1 signal measured in a window including MFP and LFP (rectangles in D,E) in control and αSulf1-treated explants. (F-H) Detection of *shh* mRNA 3 hours (F) and 2 days (G,H) after plating. Note that expression of *shh* in LFP is unaffected in αSulf1-treated explants (H). (J-K′) Immunodetection of Shh (green) and Nkx2.2 (red) in explants electroporated with *gfp*RNAi (blue in J,J′) or *sulf1*siRNA (blue in K,K′). Note weak 5E1 signal at the apical surface of *sulf1*RNAi-electroporated cells (compare K,K′ and J,J′). (L) Measurement of the 5E1 signal intensity in windows positioned over electroporated (e) and non-electroporated (ne) LFP cells (rectangles in J′,K′). Results are expressed as mean pixel intensity ± s.e.m. (***P*<0.01, **P*<0.05). VZ, ventricular zone; MZ, marginal zone; *ptc1, patched 1*. Scale bar: 50 µm.

an enhanced Shh response would be expected, but this is not the case because Sulf1 inactivation instead reduces Shh signaling in this context (Touahri et al., 2012). Therefore, we favor the second interpretation and propose that Sulf1 contributes to activate Shh signaling by stimulating production of a fully activated form of Shh from ligand source cells.

DISCUSSION

Establishment of gene expression domains in the ventral neural tube is a dynamic process resulting from the sequential emergence, at two critical time periods, of more ventral transcription codes that trigger successive generation of neurons and glial cells. Our work emphasizes the key role of Sulf1 in changing the inductive properties of Shh source cells to promote these progressive processes. We provide evidence that Sulf1 expression in Shh-producing cells is essential for correct activation of high-threshold responses to the morphogen and propose a model wherein temporal evolution of Shh source cells influences the establishment and remodeling of the ventral spinal cord patterning (Fig. 9).

Sulf1 triggers Shh-dependent generation of neuronal subtypes and OPCs at two temporally distinct stages

As in other vertebrates, Hedgehog (Hh) signaling in zebrafish is required to specify ventral neurons and, later, oligodendroglial cells. Our results, showing that Sulf1 depletion impairs generation of V3 interneurons and OPCs in the zebrafish spinal cord, confirm its requirement for OPC induction and extend the range of Sulf1 function by highlighting its role also in neuronal production. Strikingly, *sulf1*

Development (2014) doi:10.1242/dev.101717

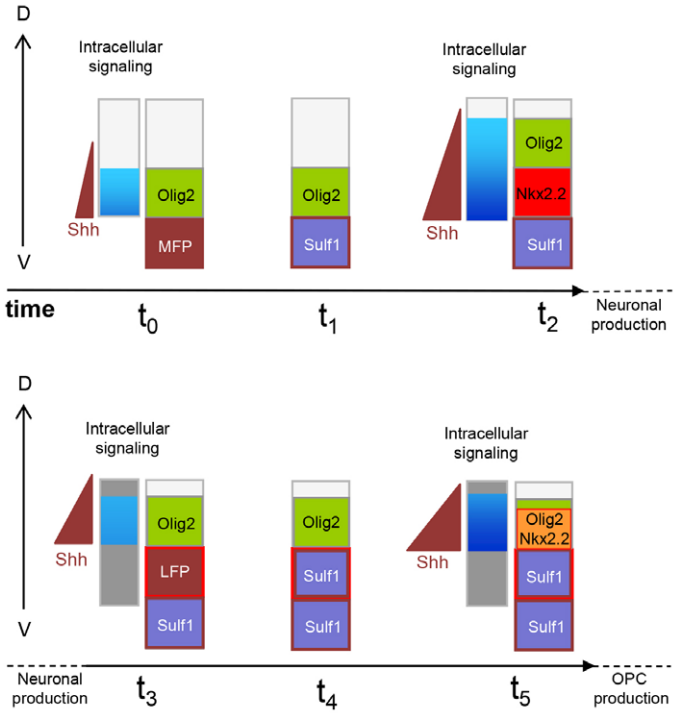

Fig. 9. Model for Sulf1 function. Scheme showing Shh-dependent gene expression at stages of patterning establishment (t_0-t_2) and rearrangement (t_3-t_5) in the ventral spinal cord. At t_0, Shh (brown) secreted by MFP cells activates low level of intracellular signaling to maintain expression of Olig2 (green) in adjacent neural progenitors. As development progresses (t_1), upregulation of Sulf1 in MFP (purple) promotes provision of active forms of Shh from its source. Nkx2.2 (red) is subsequently induced in cells adjacent to the MFP (t_2). Nkx2.2 further suppresses Olig2, leading to formation of the p3 domain from which V3 interneurons are generated. Long after patterning establishment (t_3), LFP (brown) forms in the former p3 domain. Again, upregulation of Sulf1 in LFP (purple) stimulates provision of active forms of Shh from its source (t_4). Subsequent activation of Shh signal transduction in adjacent Olig2-expressing cells induces expression of Nkx2.2. Co-expression of Nkx2.2 and Olig2 (orange) further leads to formation of the p* domain, which generates OPCs (t_5). Adapted from Balaskas et al. (Balaskas et al., 2012).

morphants fail to generate V3 interneurons but not primary MNs, both requiring Hh for their specification (England et al., 2011; Huang et al., 2012; Lewis and Eisen, 2001; Mich and Chen, 2011; Park et al., 2002; Pinheiro et al., 2004; Schäfer et al., 2007). In zebrafish, three distinct *hh* genes are expressed in different subsets of Hh source cells. In the early neural tube, MFP cells express *Shhb* (*twhh*) together with *shha*, the closest ortholog of the mammalian Shh, referred to here as *shh*, whereas *ihhb* (*ehh*), initially expressed in the notochord, is upregulated in FP cells at stages of OPC induction (Chung et al., 2013; Currie and Ingham, 1996; Ekker et al., 1995; Krauss et al., 1993). Therefore, at least two distinct ligands are produced in Hh source cells at initiation of *sulf1* expression at either neurogenic or gliogenic stages. However, although elimination of all three Hh signals prevents MN generation, *sonic-you* (*syu*) mutant embryos, lacking only *shh,* produce normal numbers of MNs (Lewis and Eisen, 2001; Park et al., 2004). Therefore, the persistent generation of MNs in *sulf1* morphants indicates that Hh activity is not completely abolished and opens the possibility that Sulf1 controls the activity of one particular Hh ligand. In support of this, *syu* embryos fail to produce OPCs whereas these cells are generated at a normal rate in *shhb* (*twhh*) morphants (Park et al., 2004). However, *ihhb* has also recently been implicated in controlling OPC generation (Chung et al., 2013), leaving this question open.

Sulf1 is required over time for neural patterning establishment and rearrangement

In amniotes, establishment of the ventral neural tube patterning depends on exposure to progressively higher Shh concentrations and longer duration of intracellular Shh signaling (Ribes and Briscoe, 2009). In zebrafish, cell sorting also contributes to refinement of the ventral patterning (Xiong et al., 2013). Our data show that the temporal sequence of *olig2* and *nkx2.2* expression in the ventral neural tube is conserved in zebrafish. However, our results reveal that MFP induction and formation of the p3 domain in zebrafish follow different schedules than in amniotes. In chicken and mouse, the ventral patterning is indeed initially influenced by an Shh gradient emanating from the notochord, and *shh* expression in the prospective MFP is induced secondarily to *nkx2.2* upregulation (Chamberlain et al., 2008; Jeong and McMahon, 2005; Lek et al., 2010; Matise et al., 1998; Ribes et al., 2010; Yu et al., 2013). In zebrafish, *shh* expression in MFP cells precedes *nkx2.2a* expression. This is in agreement with MFP induction in zebrafish mainly depending on Nodal, Hh signaling playing a less significant role (Placzek and Briscoe, 2005; Ribes et al., 2010). Therefore, the Hh source driving patterning establishment in zebrafish is likely to lie in MFP cells. In support of this, upregulation Hh-dependent *olig2* in neural plate cells coincides with s*hh* expression in MFP (Concordet et al., 1996; Park et al., 2002).

Consistent with deficient generation of V3 interneurons, *sulf1* depletion inhibits upregulation of *nkx2.2a*, which is recognized as a high-threshold Hh responsive gene. This phenotype, very reminiscent of that of *disp1* and *boc* mutant zebrafish embryos (Bergeron et al., 2011; Nakano et al., 2004), highlights the role of Sulf1 in assigning the ventral-most neural identity, acting as an enhancer of Hh signaling. It is noteworthy that *sulf1* depletion, although preventing correct temporal activation of *nkx2.2a*, does not permanently inhibit its expression, which eventually occurs but with a severe delay. Therefore, at the onset of OPC generation, the two adjacent *nkx2.2a*- and *olig2*-expressing domains are in place. As treatment of neural cells with low concentration of Shh but for a longer period of time activates the highest levels of signal transduction (Dessaud et al., 2010; Dessaud et al., 2007), one attractive interpretation of this recovery is that prolonged exposure to reduced doses of Hh is sufficient to induce *nkx2.2a* expression in *sulf1*-depleted embryos. However, despite restoration of the ventral patterning over time, OPCs failed to be induced in *sulf1*-depleted embryos because of a defective *nkx2.2a* upregulation in *olig2*-expressing progenitors. This is in agreement with our previous data showing that, in chicken, downregulation of Sulf1 just prior to patterning rearrangement prevents formation of the p* domain (Touahri et al., 2012), supporting the view that the early function of Sulf1 in stimulating Shh activity is not sufficient for this later event. Therefore, Sulf1 is a key player in controlling cell fate diversification, acting as a timer to activate a high-threshold response to Hh at two distinct developmental stages.

Sulf1 acts at the ligand source to stimulate Hh signaling activity in neighboring cells

Our data provided evidence that *sulf1* expression is restricted to Hh-producing cells. Therefore, they highlight a novel mechanism involved in the temporal control of Hh signaling, lying at the ligand source. Because in zebrafish extensive cell movements occur in the early neural tube (Xiong et al., 2013), it is worth noting that *sulf1*

Development (2014) doi:10.1242/dev.101717

expression in MFP cells starts when these movements slowed down (14/15 hpf) and when a clear gradient of Hh activity is apparent in the ventral neural tube. Therefore, Sulf1 regulates establishment of the ventral patterning when cells have acquired a stable position relative to the Hh source. Importantly, although *shh* and *sulf1* expression patterns have a similar spatial organization, initiation of *sulf1* expression is invariably delayed compared with that of *shh*. In particular, *sulf1* upregulation in Hh source cells reiteratively occurs immediately prior to assignment of a *nkx2.2a* identity to neighboring cells. Furthermore, our data unambiguously show that MFP or LFP formation is not sufficient per se to activate expression of high Hh responsive genes at the correct time; instead Hh-expressing cells must express *sulf1* to reach their full inductive potential. Shh is well known to interact with heparan sulfate (HS) chains and to preferentially bind HS chains having a high level of sulfation (Carrasco et al., 2005; Chang et al., 2011; Dierker et al., 2009; Farshi et al., 2011; Zhang et al., 2007). Therefore, as reported for other signaling molecules (Ai et al., 2003; Freeman et al., 2008; Viviano et al., 2004), Sulf1 activity is likely to lower Shh-HSPG interaction. An attractive hypothesis is that Sulf1 stimulates Shh signaling by simply promoting release of a diffusible form of Shh free to travel dorsally. Requirement of a greater amount of Shh ligand for correct *nkx2.2a* induction is indeed supported by our cyclopamine data showing that partial inhibition of the Shh co-receptor Smo, at stages of *sulf1* upregulation, is sufficient to prevent *nkx2.2a* expression. According to this hypothesis, Sulf1-depleted Shh source cells would be expected to retain Shh at their surface as a result of increased abundance of 6O-sulfated HSPGs displaying higher affinity for Shh. However, our data did not reveal such an accumulation and, instead, showed that Sulf1 inactivation reduces the amount of the 5E1-immunoreactive form of Shh. Although these data do not preclude accumulation of an immature form of Shh at the source, they do highlight the involvement of Sulf1 in controlling production of a fully active form of Shh, a process known to depend on HSPGs (Briscoe and Thérond, 2013; Gradilla and Guerrero, 2013; Thérond, 2012). In agreement with this idea, overexpression of Sulf1, although stimulating Shh signaling, increases the density of 5E1-immunoreactive punctae in the chicken ventral spinal cord (Danesin et al., 2006). Keeping in mind that the enzyme is secreted and that HSPGs are key players in regulating Shh stability, retention and binding to its receptors (Briscoe and Thérond, 2013; Gradilla and Guerrero, 2013; Thérond, 2012), the possibility that Sulf1 also regulates signal reception to provide higher level/longer duration of Shh signaling cannot be excluded. However, in *Drosophila*, when expressed in the Hh-receiving field, Sulf1 does not stimulate Hh signaling, but, on the contrary, reduces the response to the morphogen (Wojcinski et al., 2011). Accordingly, loss of Shh-HSPG interaction has been reported to reduce Shh signaling potency *in vitro* (Chang et al., 2011). These data, together with our present results showing that Sulf1 invariably activates Shh signaling in the neural tube, argue against Sulf1 acting in the immediate environment of Shh-receiving cells.

Overall, our work, by characterizing Sulf1 as a major player in controlling generation of neural cell diversity in response to Shh, highlights a novel level of regulation that involves temporal evolution of Shh source properties over spinal cord development.

MATERIALS AND METHODS

Animals

Animal procedures were performed according to the EC guiding principles (86/609/CEE), French Decree no. 97/748 and the recommendations of the Centre National de la Recherche Scientifique (CNRS).

Zebrafish

Embryos were staged according to standard protocols (Kimmel et al., 1995). *Sulf1*$^{sa199-/-}$ embryos (Zebrafish Mutation Project) were obtained by intercrossing *sulf1*$^{sa199+/-}$ carriers. Genotyping was performed using the following primers: 5′-GCCAGATCCCTGTCAGTCGAGTTT-3′ and 5′-TCGAGGCTTACTTGTGGGTGACTT-3′ (Eurofin MWG Operon). *Tg(olig2:egfp)vu12* (Shin et al., 2003), *Tg(nkx2.2a:mEGFP)vu17* (Kirby et al., 2006) and *Tg(olig2:dsRed2)vu19* (Kucenas et al., 2008b) transgenic lines were used to visualize OPCs. The *Tg(shh:EGFP)* line (Shkumatava et al., 2004) was used to monitor *shh* expression. Morpholino (MO) and mRNA injections were performed in one- or two-cell stage embryos. The following MOs (Gene Tools, LLC) were used: *sulf1*MO^{ATG} (5′-AACGCGAATCAG-AAGGTTGGAATCC-3′; 34 ng/embryo), *sulf1*MO^{splice} (5′-ATTGCATCTG-GTCTACTCACCCAAC-3′; 22 ng/embryo), *sulf1* mismatch MO (5′-AACGgGAATgAGAAcGTTcGAATgC-3′; 20 ng/embryo) and standard control MO targeting the human β-globin (ctrlMO, 34 ng/embryo). Rescue experiments were performed by co-injection of *sulf1*MO^{splice} (22 ng) and *sulf1* mRNA (450 pg), as previously reported (Gorsi et al., 2013). For cyclopamine (Enzo Life Sciences) treatments, embryos ($n \geq 10$ for each experimental condition) were incubated in fish water supplemented with the drug.

Whole-mount *in situ* hybridization (ISH) was performed as described previously (Macdonald et al., 1994) using the following RNA probes: *sulf1* (Gorsi et al., 2010), *nkx2.2a* (Barth and Wilson, 1995), *nkx2.9* (Guner and Karlstrom, 2007), *olig2* (Park et al., 2002), *plp*/*dm20* (Park et al., 2002), *foxa2* (Strähle et al., 1993), *shh* (Krauss et al., 1993), *arx* (Miura et al., 1997), *pax7a* (Seo et al., 1998), *ptc1* (Concordet et al., 1996), *pax2a* (Pfeffer et al., 1998), *islet2a* (Appel et al., 1995), *tal2* (Pinheiro et al., 2004), *sim1* (Serluca and Fishman, 2001) and *mbpa* (Brösamle and Halpern, 2002). After ISH, embryos were embedded in gelatine/albumin and 10-15 µm sections were cut using a vibratome (Leica VT1000s). Rabbit anti-GFP (1/500, Torrey Pines Biolabs) and Alexa Fluor 488-conjugated goat anti-rabbit IgG (1/1000, Molecular Probes) were used to detect GFP on whole-mount transgenic embryos.

Chicken and mouse

Staging, genotyping and processing of mouse embryos were performed according to Touahri et al. (Touahri et al., 2012). Chicken eggs were incubated at 38°C and staged according to Hamburger and Hamilton (Hamburger and Hamilton, 1992). Electroporation of *sulf1*RNAi (Touahri et al., 2012) and *gfp*RNAi (Das et al., 2006) expression vectors was performed as previously reported (Touahri et al., 2012). Organotypic culture of flat-mount spinal cord explants was performed as previously described (Agius et al., 2004). Sulf1-neutralizing antibody (αSulf1) was used at 1/50 dilution (Touahri et al., 2012). ISH and immunostainings were performed on 60-80 µm vibratome sections (Braquart-Varnier et al., 2004; Danesin et al., 2006), using a chick probe for *shh* (Marigo and Tabin, 1996) and the following antibodies: rabbit anti-GFP (1/500; Torrey Pines Scientific), anti-Olig2 (1/500; Millipore), anti-Sulf1 (1/200) (Touahri et al., 2012), anti-Shh [5E1, 1/8 (Ericson et al., 1996)], anti-Nkx2.2 [1/2 (Ericson et al., 1997)], Alexa Fluor 488, 555 or 647 secondary antibodies (1/500, Molecular Probes). After detection of Shh in living chick explants (Danesin et al., 2006), tissues were fixed, sectioned and processed for Nkx2.2 and/or Olig2 immunostaining using standard procedures.

Imaging, cell counting and statistical analysis

Images of ISHs were collected with Nikon digital camera DXM1200C and a Nikon eclipse 80*i* microscope. Fluorescence photomicrographs were collected with Leica SP5 and Zeiss 710 confocal microscopes. Images were processed using Adobe Photoshop CS2. Cells were counted in zebrafish between somites 14 and 18 on at least three embryos from at least two independent experiments. Statistical analyses were performed using the Mann-Whitney U-test. Pixel quantification for 5E1 immunostaining was performed using ImageJ and Excel software. Integrated pixel density was measured on optical sections within a 140×20 µm window including MFP and LFP for αSulf1-treated explants and in a 70×10 µm window positioned over the LFP for electroporation assays. Quantification was performed on at least three tissue slices per explant. For each tissue slice, at least three optical

sections (8 μm intervals) were acquired and analyzed. Data are an average of at least five explants from at least two independent experiments. Statistical analysis was performed using the Mann-Whitney U-test for Sulf1-blocking antibody experiments and a Wilcoxon matched paired-test for comparing electroporated and non-electroporated sides of explants. $P<0.05$ was considered statistically significant.

Acknowledgements

We acknowledge the Zebrafish Mutation Project (Sanger Institute) and the European Zebrafish Resource Center for generating and distributing *sulf1* mutant line. We are grateful to Developmental Studies Hybridoma Bank (Iowa City, IA, USA), for supplying monoclonal antibodies. We thank B. Appel, S. Temple, C. Winkler, P. Blader, U. Strahle, C. Houart and R. Karlstrom for sharing transgenic lines and reagents; F. Pituello and E. Cau for critical reading of the manuscript; S. Relexans and J. Auriol for zebrafish and mouse care, respectively; and the Toulouse Regional Imaging Platform for technical assistance in confocal microscopy.

Competing interests

The authors declare no competing financial interests.

Author contributions

C.D. and C.S. conceived experiments and wrote the paper. A.A.O., B.G., C.D., N.K.-F., M.-A.F., N.E. and P.C. performed experiments and analyzed the data.

Funding

This work was supported by the Agence Nationale de la Recherche; the Fondation pour l'Aide à la Recherche sur la Sclérose En Plaques; the Centre National de la Recherche Scientifique; and the University of Toulouse. A.A.O. and M.-A.F. were supported by grants from the French Ministry of National Education, Research, and Technology.

Supplementary material

Supplementary material available online at
http://dev.biologists.org/lookup/suppl/doi:10.1242/dev.101717/-/DC1

References

Agius, E., Soukkarieh, C., Danesin, C., Kan, P., Takebayashi, H., Soula, C. and Cochard, P. (2004). Converse control of oligodendrocyte and astrocyte lineage development by Sonic hedgehog in the chick spinal cord. *Dev. Biol.* **270**, 308-321.

Ai, X., Do, A. T., Lozynska, O., Kusche-Gullberg, M., Lindahl, U. and Emerson, C. P., Jr (2003). QSulf1 remodels the 6-O sulfation states of cell surface heparan sulfate proteoglycans to promote Wnt signaling. *J. Cell Biol.* **162**, 341-351.

Ai, X., Do, A. T., Kusche-Gullberg, M., Lindahl, U., Lu, K. and Emerson, C. P., Jr (2006). Substrate specificity and domain functions of extracellular heparan sulfate 6-O-endosulfatases, QSulf1 and QSulf2. *J. Biol. Chem.* **281**, 4969-4976.

Allen, B. L., Song, J. Y., Izzi, L., Althaus, I. W., Kang, J. S., Charron, F., Krauss, R. S. and McMahon, A. P. (2011). Overlapping roles and collective requirement for the coreceptors GAS1, CDO, and BOC in SHH pathway function. *Dev. Cell* **20**, 775-787.

Appel, B., Korzh, V., Glasgow, E., Thor, S., Edlund, T., Dawid, I. B. and Eisen, J. S. (1995). Motoneuron fate specification revealed by patterned LIM homeobox gene expression in embryonic zebrafish. *Development* **121**, 4117-4125.

Balaskas, N., Ribeiro, A., Panovska, J., Dessaud, E., Sasai, N., Page, K. M., Briscoe, J. and Ribes, V. (2012). Gene regulatory logic for reading the Sonic Hedgehog signaling gradient in the vertebrate neural tube. *Cell* **148**, 273-284.

Barth, K. A. and Wilson, S. W. (1995). Expression of zebrafish nk2.2 is influenced by sonic hedgehog/vertebrate hedgehog-1 and demarcates a zone of neuronal differentiation in the embryonic forebrain. *Development* **121**, 1755-1768.

Bergeron, S. A., Tyurina, O. V., Miller, E., Bagas, A. and Karlstrom, R. O. (2011). Brother of cdo (umleitung) is cell-autonomously required for Hedgehog-mediated ventral CNS patterning in the zebrafish. *Development* **138**, 75-85.

Bishop, B., Aricescu, A. R., Harlos, K., O'Callaghan, C. A., Jones, E. Y. and Siebold, C. (2009). Structural insights into hedgehog ligand sequestration by the human hedgehog-interacting protein HHIP. *Nat. Struct. Mol. Biol.* **16**, 698-703.

Bosanac, I., Maun, H. R., Scales, S. J., Wen, X., Lingel, A., Bazan, J. F., de Sauvage, F. J., Hymowitz, S. G. and Lazarus, R. A. (2009). The structure of SHH in complex with HHIP reveals a recognition role for the Shh pseudo active site in signaling. *Nat. Struct. Mol. Biol.* **16**, 691-697.

Braquart-Varnier, C., Danesin, C., Clouscard-Martinato, C., Agius, E., Escalas, N., Benazeraf, B., Ai, X., Emerson, C., Cochard, P. and Soula, C. (2004). A subtractive approach to characterize genes with regionalized expression in the gliogenic ventral neuroepithelium: identification of chick sulfatase 1 as a new oligodendrocyte lineage gene. *Mol. Cell. Neurosci.* **25**, 612-628.

Briscoe, J. and Thérond, P. P. (2013). The mechanisms of Hedgehog signalling and its roles in development and disease. *Nat. Rev. Mol. Cell Biol.* **14**, 416-429.

Brösamle, C. and Halpern, M. E. (2002). Characterization of myelination in the developing zebrafish. *Glia* **39**, 47-57.

Carrasco, H., Olivares, G. H., Faunes, F., Oliva, C. and Larraín, J. (2005). Heparan sulfate proteoglycans exert positive and negative effects in Shh activity. *J. Cell. Biochem.* **96**, 831-838.

Chamberlain, C. E., Jeong, J., Guo, C., Allen, B. L. and McMahon, A. P. (2008). Notochord-derived Shh concentrates in close association with the apically positioned basal body in neural target cells and forms a dynamic gradient during neural patterning. *Development* **135**, 1097-1106.

Chang, S. C., Mulloy, B., Magee, A. I. and Couchman, J. R. (2011). Two distinct sites in sonic Hedgehog combine for heparan sulfate interactions and cell signaling functions. *J. Biol. Chem.* **286**, 44391-44402.

Charrier, J. B., Lapointe, F., Le Douarin, N. M. and Teillet, M. A. (2002). Dual origin of the floor plate in the avian embryo. *Development* **129**, 4785-4796.

Chung, A. Y., Kim, S., Kim, E., Kim, D., Jeong, I., Cha, Y. R., Bae, Y. K., Park, S. W., Lee, J. and Park, H. C. (2013). Indian hedgehog B function is required for the specification of oligodendrocyte progenitor cells in the zebrafish CNS. *J. Neurosci.* **33**, 1728-1733.

Concordet, J. P., Lewis, K. E., Moore, J. W., Goodrich, L. V., Johnson, R. L., Scott, M. P. and Ingham, P. W. (1996). Spatial regulation of a zebrafish patched homologue reflects the roles of sonic hedgehog and protein kinase A in neural tube and somite patterning. *Development* **122**, 2835-2846.

Cooper, M. K., Porter, J. A., Young, K. E. and Beachy, P. A. (1998). Teratogen-mediated inhibition of target tissue response to Shh signaling. *Science* **280**, 1603-1607.

Currie, P. D. and Ingham, P. W. (1996). Induction of a specific muscle cell type by a hedgehog-like protein in zebrafish. *Nature* **382**, 452-455.

Danesin, C., Agius, E., Escalas, N., Ai, X., Emerson, C., Cochard, P. and Soula, C. (2006). Ventral neural progenitors switch toward an oligodendroglial fate in response to increased Sonic hedgehog (Shh) activity: involvement of Sulfatase 1 in modulating Shh signaling in the ventral spinal cord. *J. Neurosci.* **26**, 5037-5048.

Das, R. M., Van Hateren, N. J., Howell, G. R., Farrell, E. R., Bangs, F. K., Porteous, V. C., Manning, E. M., McGrew, M. J., Ohyama, K., Sacco, M. A. et al. (2006). A robust system for RNA interference in the chicken using a modified microRNA operon. *Dev. Biol.* **294**, 554-563.

Dessaud, E., Yang, L. L., Hill, K., Cox, B., Ulloa, F., Ribeiro, A., Mynett, A., Novitch, B. G. and Briscoe, J. (2007). Interpretation of the sonic hedgehog morphogen gradient by a temporal adaptation mechanism. *Nature* **450**, 717-720.

Dessaud, E., Ribes, V., Balaskas, N., Yang, L. L., Pierani, A., Kicheva, A., Novitch, B. G., Briscoe, J. and Sasai, N. (2010). Dynamic assignment and maintenance of positional identity in the ventral neural tube by the morphogen sonic hedgehog. *PLoS Biol.* **8**, e1000382.

Dhoot, G. K., Gustafsson, M. K., Ai, X., Sun, W., Standiford, D. M. and Emerson, C. P., Jr (2001). Regulation of Wnt signaling and embryo patterning by an extracellular sulfatase. *Science* **293**, 1663-1666.

Dierker, T., Dreier, R., Petersen, A., Bordych, C. and Grobe, K. (2009). Heparan sulfate-modulated, metalloprotease-mediated sonic hedgehog release from producing cells. *J. Biol. Chem.* **284**, 8013-8022.

Ekker, S. C., Ungar, A. R., Greenstein, P., von Kessler, D. P., Porter, J. A., Moon, R. T. and Beachy, P. A. (1995). Patterning activities of vertebrate hedgehog proteins in the developing eye and brain. *Curr. Biol.* **5**, 944-955.

England, S., Batista, M. F., Mich, J. K., Chen, J. K. and Lewis, K. E. (2011). Roles of Hedgehog pathway components and retinoic acid signalling in specifying zebrafish ventral spinal cord neurons. *Development* **138**, 5121-5134.

Ericson, J., Morton, S., Kawakami, A., Roelink, H. and Jessell, T. M. (1996). Two critical periods of Sonic Hedgehog signaling required for the specification of motor neuron identity. *Cell* **87**, 661-673.

Ericson, J., Rashbass, P., Schedl, A., Brenner-Morton, S., Kawakami, A., van Heyningen, V., Jessell, T. M. and Briscoe, J. (1997). Pax6 controls progenitor cell identity and neuronal fate in response to graded Shh signaling. *Cell* **90**, 169-180.

Farshi, P., Ohlig, S., Pickhinke, U., Höing, S., Jochmann, K., Lawrence, R., Dreier, R., Dierker, T. and Grobe, K. (2011). Dual roles of the Cardin-Weintraub motif in multimeric Sonic hedgehog. *J. Biol. Chem.* **286**, 23608-23619.

Freeman, S. D., Moore, W. M., Guiral, E. C., Holme, A. D., Turnbull, J. E. and Pownall, M. E. (2008). Extracellular regulation of developmental cell signaling by XtSulf1. *Dev. Biol.* **320**, 436-445.

Fu, H., Qi, Y., Tan, M., Cai, J., Takebayashi, H., Nakafuku, M., Richardson, W. and Qiu, M. (2002). Dual origin of spinal oligodendrocyte progenitors and evidence for the cooperative role of Olig2 and Nkx2.2 in the control of oligodendrocyte differentiation. *Development* **129**, 681-693.

Gorsi, B., Whelan, S. and Stringer, S. E. (2010). Dynamic expression patterns of 6-O endosulfatases during zebrafish development suggest a subfunctionalisation event for sulf2. *Dev. Dyn.* **239**, 3312-3323.

Gorsi, B., Liu, F., Ma, X., Chico, T. J., Shrinivasan, A., Kramer, K. L., Bridges, E., Monteiro, R., Harris, A. L., Patient, R. et al. (2013). The heparan sulfate editing enzyme Sulf1 plays a novel role in zebrafish VegfA mediated arterial venous identity. *Angiogenesis*.

Gradilla, A. C. and Guerrero, I. (2013). Hedgehog on the move: a precise spatial control of Hedgehog dispersion shapes the gradient. *Curr. Opin. Genet. Dev.* **23**, 363-373.

Guner, B. and Karlstrom, R. O. (2007). Cloning of zebrafish nkx6.2 and a comprehensive analysis of the conserved transcriptional response to Hedgehog/Gli signaling in the zebrafish neural tube. *Gene Expr. Patterns* **7**, 596-605.

Huang, P., Xiong, F., Megason, S. G. and Schier, A. F. (2012). Attenuation of Notch and Hedgehog signaling is required for fate specification in the spinal cord. *PLoS Genet.* **8**, e1002762.

Incardona, J. P., Gaffield, W., Kapur, R. P. and Roelink, H. (1998). The teratogenic Veratrum alkaloid cyclopamine inhibits sonic hedgehog signal transduction. *Development* **125**, 3553-3562.
Jeong, J. and McMahon, A. P. (2005). Growth and pattern of the mammalian neural tube are governed by partially overlapping feedback activities of the hedgehog antagonists patched 1 and Hhip1. *Development* **132**, 143-154.
Jessell, T. M. (2000). Neuronal specification in the spinal cord: inductive signals and transcriptional codes. *Nat. Rev. Genet.* **1**, 20-29.
Kimmel, C. B., Ballard, W. W., Kimmel, S. R., Ullmann, B. and Schilling, T. F. (1995). Stages of embryonic development of the zebrafish. *Dev. Dyn.* **203**, 253-310.
Kirby, B. B., Takada, N., Latimer, A. J., Shin, J., Carney, T. J., Kelsh, R. N. and Appel, B. (2006). In vivo time-lapse imaging shows dynamic oligodendrocyte progenitor behavior during zebrafish development. *Nat. Neurosci.* **9**, 1506-1511.
Krauss, S., Concordet, J. P. and Ingham, P. W. (1993). A functionally conserved homolog of the Drosophila segment polarity gene hh is expressed in tissues with polarizing activity in zebrafish embryos. *Cell* **75**, 1431-1444.
Kucenas, S., Snell, H. and Appel, B. (2008a). nkx2.2a promotes specification and differentiation of a myelinating subset of oligodendrocyte lineage cells in zebrafish. *Neuron Glia Biol.* **4**, 71-81.
Kucenas, S., Takada, N., Park, H. C., Woodruff, E., Broadie, K. and Appel, B. (2008b). CNS-derived glia ensheath peripheral nerves and mediate motor root development. *Nat. Neurosci.* **11**, 143-151.
Lamanna, W. C., Kalus, I., Padva, M., Baldwin, R. J., Merry, C. L. and Dierks, T. (2007). The heparanome – the enigma of encoding and decoding heparan sulfate sulfation. *J. Biotechnol.* **129**, 290-307.
Lek, M., Dias, J. M., Marklund, U., Uhde, C. W., Kurdija, S., Lei, Q., Sussel, L., Rubenstein, J. L., Matise, M. P., Arnold, H. H. et al. (2010). A homeodomain feedback circuit underlies step-function interpretation of a Shh morphogen gradient during ventral neural patterning. *Development* **137**, 4051-4060.
Lewis, K. E. and Eisen, J. S. (2001). Hedgehog signaling is required for primary motoneuron induction in zebrafish. *Development* **128**, 3485-3495.
Macdonald, R., Xu, Q., Barth, K. A., Mikkola, I., Holder, N., Fjose, A., Krauss, S. and Wilson, S. W. (1994). Regulatory gene expression boundaries demarcate sites of neuronal differentiation in the embryonic zebrafish forebrain. *Neuron* **13**, 1039-1053.
Marigo, V. and Tabin, C. J. (1996). Regulation of patched by sonic hedgehog in the developing neural tube. *Proc. Natl. Acad. Sci. USA* **93**, 9346-9351.
Matise, M. P., Epstein, D. J., Park, H. L., Platt, K. A. and Joyner, A. L. (1998). Gli2 is required for induction of floor plate and adjacent cells, but not most ventral neurons in the mouse central nervous system. *Development* **125**, 2759-2770.
Maun, H. R., Wen, X., Lingel, A., de Sauvage, F. J., Lazarus, R. A., Scales, S. J. and Hymowitz, S. G. (2010). Hedgehog pathway antagonist 5E1 binds hedgehog at the pseudo-active site. *J. Biol. Chem.* **285**, 26570-26580.
Meyers, J. R., Planamento, J., Ebrom, P., Krulewitz, N., Wade, E. and Pownall, M. E. (2013). Sulf1 modulates BMP signaling and is required for somite morphogenesis and development of the horizontal myoseptum. *Dev. Biol.* **378**, 107-121.
Mich, J. K. and Chen, J. K. (2011). Hedgehog and retinoic acid signaling cooperate to promote motoneurogenesis in zebrafish. *Development* **138**, 5113-5119.
Miura, H., Yanazawa, M., Kato, K. and Kitamura, K. (1997). Expression of a novel aristaless related homeobox gene 'Arx' in the vertebrate telencephalon, diencephalon and floor plate. *Mech. Dev.* **65**, 99-109.
Myers, P. Z., Eisen, J. S. and Westerfield, M. (1986). Development and axonal outgrowth of identified motoneurons in the zebrafish. *J. Neurosci.* **6**, 2278-2289.
Nakano, Y., Kim, H. R., Kawakami, A., Roy, S., Schier, A. F. and Ingham, P. W. (2004). Inactivation of dispatched 1 by the chameleon mutation disrupts Hedgehog signalling in the zebrafish embryo. *Dev. Biol.* **269**, 381-392.
Norton, W. H., Mangoli, M., Lele, Z., Pogoda, H. M., Diamond, B., Mercurio, S., Russell, C., Teraoka, H., Stickney, H. L., Rauch, G. J. et al. (2005). Monorail/Foxa2 regulates floorplate differentiation and specification of oligodendrocytes, serotonergic raphé neurones and cranial motoneurones. *Development* **132**, 645-658.
Odenthal, J., van Eeden, F. J., Haffter, P., Ingham, P. W. and Nüsslein-Volhard, C. (2000). Two distinct cell populations in the floor plate of the zebrafish are induced by different pathways. *Dev. Biol.* **219**, 350-363.
Park, H. C., Mehta, A., Richardson, J. S. and Appel, B. (2002). olig2 is required for zebrafish primary motor neuron and oligodendrocyte development. *Dev. Biol.* **248**, 356-368.
Park, H. C., Shin, J. and Appel, B. (2004). Spatial and temporal regulation of ventral spinal cord precursor specification by Hedgehog signaling. *Development* **131**, 5959-5969.
Pfeffer, P. L., Gerster, T., Lun, K., Brand, M. and Busslinger, M. (1998). Characterization of three novel members of the zebrafish Pax2/5/8 family: dependency of Pax5 and Pax8 expression on the Pax2.1 (noi) function. *Development* **125**, 3063-3074.
Pinheiro, P., Gering, M. and Patient, R. (2004). The basic helix-loop-helix transcription factor, Tal2, marks the lateral floor plate of the spinal cord in zebrafish. *Gene Expr. Patterns* **4**, 85-92.
Placzek, M. and Briscoe, J. (2005). The floor plate: multiple cells, multiple signals. *Nat. Rev. Neurosci.* **6**, 230-240.
Ribes, V. and Briscoe, J. (2009). Establishing and interpreting graded Sonic Hedgehog signaling during vertebrate neural tube patterning: the role of negative feedback. *Cold Spring Harb. Perspect. Biol.* **1**, a002014.
Ribes, V., Balaskas, N., Sasai, N., Cruz, C., Dessaud, E., Cayuso, J., Tozer, S., Yang, L. L., Novitch, B., Marti, E. et al. (2010). Distinct Sonic Hedgehog signaling dynamics specify floor plate and ventral neuronal progenitors in the vertebrate neural tube. *Genes Dev.* **24**, 1186-1200.
Rowitch, D. H. and Kriegstein, A. R. (2010). Developmental genetics of vertebrate glial-cell specification. *Nature* **468**, 214-222.
Schäfer, M., Kinzel, D. and Winkler, C. (2007). Discontinuous organization and specification of the lateral floor plate in zebrafish. *Dev. Biol.* **301**, 117-129.
Seo, H. C., Saetre, B. O., Håvik, B., Ellingsen, S. and Fjose, A. (1998). The zebrafish Pax3 and Pax7 homologues are highly conserved, encode multiple isoforms and show dynamic segment-like expression in the developing brain. *Mech. Dev.* **70**, 49-63.
Serluca, F. C. and Fishman, M. C. (2001). Pre-pattern in the pronephric kidney field of zebrafish. *Development* **128**, 2233-2241.
Shin, J., Park, H. C., Topczewska, J. M., Mawdsley, D. J. and Appel, B. (2003). Neural cell fate analysis in zebrafish using olig2 BAC transgenics. *Methods Cell Sci.* **25**, 7-14.
Shkumatava, A., Fischer, S., Müller, F., Strahle, U. and Neumann, C. J. (2004). Sonic hedgehog, secreted by amacrine cells, acts as a short-range signal to direct differentiation and lamination in the zebrafish retina. *Development* **131**, 3849-3858.
Stamataki, D., Ulloa, F., Tsoni, S. V., Mynett, A. and Briscoe, J. (2005). A gradient of Gli activity mediates graded Sonic Hedgehog signaling in the neural tube. *Genes Dev.* **19**, 626-641.
Strähle, U., Blader, P., Henrique, D. and Ingham, P. W. (1993). Axial, a zebrafish gene expressed along the developing body axis, shows altered expression in cyclops mutant embryos. *Genes Dev.* **7B**, 1436-1446.
Thérond, P. P. (2012). Release and transportation of Hedgehog molecules. *Curr. Opin. Cell Biol.* **24**, 173-180.
Touahri, Y., Escalas, N., Benazeraf, B., Cochard, P., Danesin, C. and Soula, C. (2012). Sulfatase 1 promotes the motor neuron-to-oligodendrocyte fate switch by activating Shh signaling in Olig2 progenitors of the embryonic ventral spinal cord. *J. Neurosci.* **32**, 18018-18034.
Viviano, B. L., Paine-Saunders, S., Gasiunas, N., Gallagher, J. and Saunders, S. (2004). Domain-specific modification of heparan sulfate by Qsulf1 modulates the binding of the bone morphogenetic protein antagonist Noggin. *J. Biol. Chem.* **279**, 5604-5611.
Wang, S., Ai, X., Freeman, S. D., Pownall, M. E., Lu, Q., Kessler, D. S. and Emerson, C. P., Jr (2004). QSulf1, a heparan sulfate 6-O-endosulfatase, inhibits fibroblast growth factor signaling in mesoderm induction and angiogenesis. *Proc. Natl. Acad. Sci. USA* **101**, 4833-4838.
Wojcinski, A., Nakato, H., Soula, C. and Glise, B. (2011). DSulfatase-1 fine-tunes Hedgehog patterning activity through a novel regulatory feedback loop. *Dev. Biol.* **358**, 168-180.
Xiong, F., Tentner, A. R., Huang, P., Gelas, A., Mosaliganti, K. R., Souhait, L., Rannou, N., Swinburne, I. A., Obholzer, N. D., Cowgill, P. D. et al. (2013). Specified neural progenitors sort to form sharp domains after noisy Shh signaling. *Cell* **153**, 550-561.
Xu, J., Srinivas, B. P., Tay, S. Y., Mak, A., Yu, X., Lee, S. G., Yang, H., Govindarajan, K. R., Leong, B., Bourque, G. et al. (2006). Genomewide expression profiling in the zebrafish embryo identifies target genes regulated by Hedgehog signaling during vertebrate development. *Genetics* **174**, 735-752.
Yang, L., Rastegar, S. and Strähle, U. (2010). Regulatory interactions specifying Kolmer-Agduhr interneurons. *Development* **137**, 2713-2722.
Yu, K., McGlynn, S. and Matise, M. P. (2013). Floor plate-derived sonic hedgehog regulates glial and ependymal cell fates in the developing spinal cord. *Development* **140**, 1594-1604.
Zhang, F., McLellan, J. S., Ayala, A. M., Leahy, D. J. and Linhardt, R. J. (2007). Kinetic and structural studies on interactions between heparin or heparan sulfate and proteins of the hedgehog signaling pathway. *Biochemistry* **46**, 3933-3941.
Zhou, Q., Choi, G. and Anderson, D. J. (2001). The bHLH transcription factor Olig2 promotes oligodendrocyte differentiation in collaboration with Nkx2.2. *Neuron* **31**, 791-807.

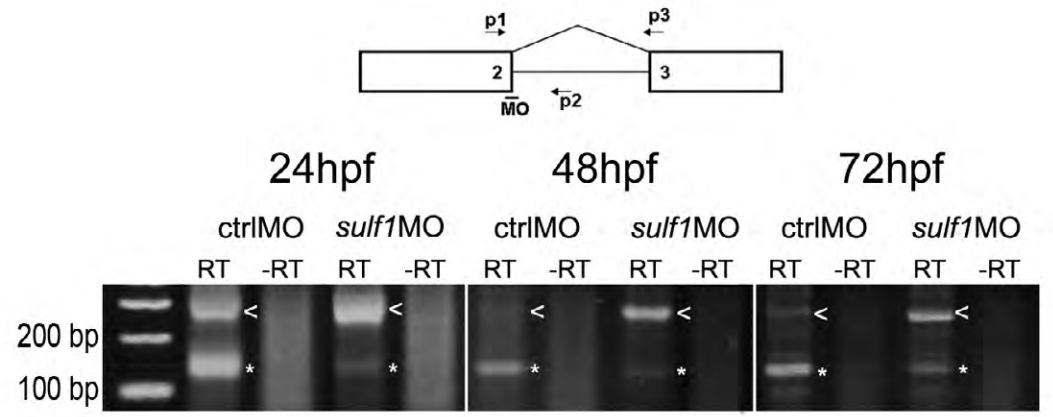

Figure S1. Efficient *sulf1* knockdown until 72 hpf in *sulf1*MO^{splice}-injected embryos. Efficacy of *sulf1* knockdown was controlled by RT-PCR at 24, 48 and 72hpf in embryos injected with *sulf1*MO^{splice} which targets the exon 2 splice donor site. RT-PCR experiments were performed using a mix of three primers, p1 (5'-CAGATGACCAGGATGTGGAG-3'), p2 (5'-CCCATCCAAATCAGTGAAGG-3') and p3 (5'-AGGATCGTGAAGGACAGCAC-3'), whose positions relative to the exon 2 splice donor site are indicated on the scheme. A PCR product of 129bp obtained using primers p1-p3 evidences *sulf1* mRNA splicing (star) while a 261bp sized PCR product obtained using primers p1-p2 evidences un-spliced forms of *sulf1* pre-mRNA (arrowheads). As indicated on upper lanes, at each stage, ctrlMO or *sulf-1*MO^{splice}-injected embryos were compared and PCR reactions were controlled on RNA extracts (-RT). Note impairment of *sulf1* mRNA splicing until 72 hpf in *sulf1*MO^{splice}-injected larvae.

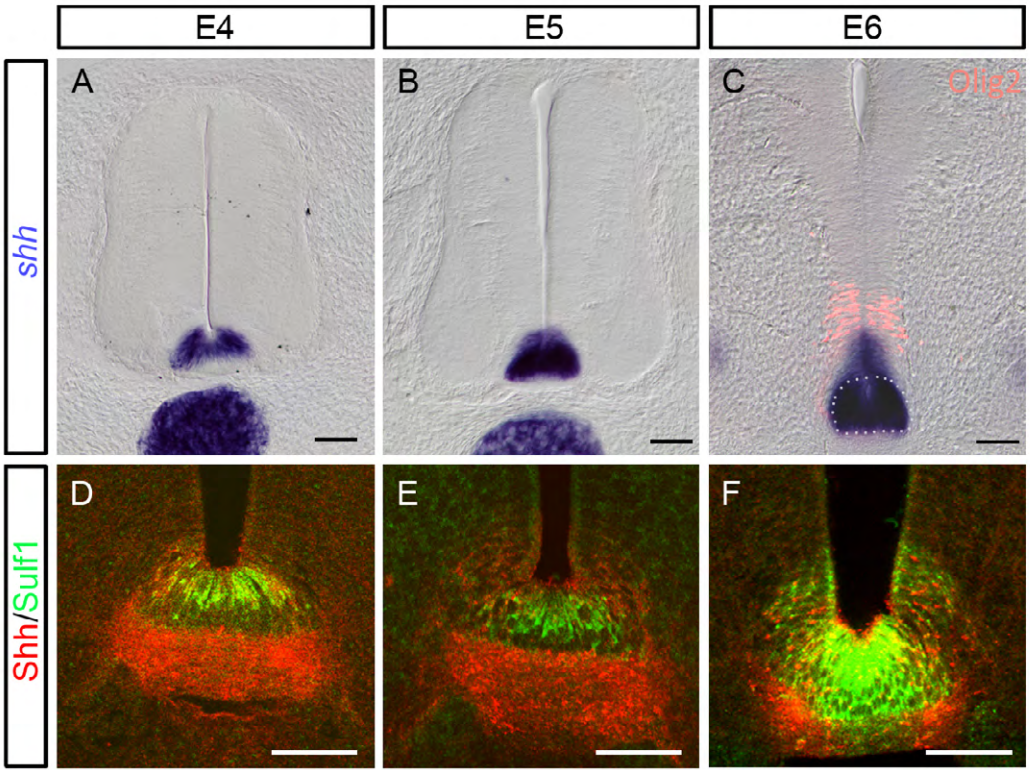

Figure S2. LFP formation and up-regulation of Sulf1 in these cells precede patterning rearrangement also in chicken. (**A-C**) Expression of *shh* on transverse sections of E4 (A), E5 (B) and E6 (C) chicken spinal cord. *Shh* expression is restricted to MFP cells at E4 (A), expands dorsally from E5 (B) and reaches the ventral border of the Olig2+ domain (red) at E6 (C), forming the LFP. Dashed line in C outlines MFP cells. (**D-F**) Double detection of Sulf1 (green) and Shh (red) on transverse sections of E4 (D), E5 (E) and E6 (F) chicken spinal cord. At E4, Sulf1 and Shh proteins are detected in MFP cells (D). At E5, Shh but not Sulf1 is detected in neural cells abutting the MFP (E). At E6, both Shh and Sulf1 are expressed in LFP cells. Scale bar = 50µm.

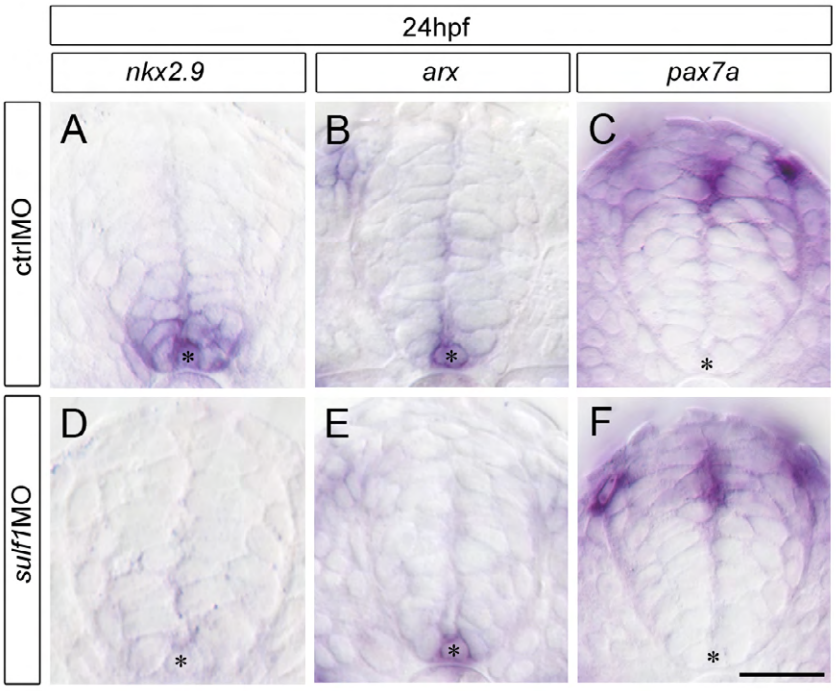

Figure S3. *Sulf1* depletion prevents up-regulation of *nkx2.9* at 24hpf without affecting expression of *arx* and *pax7* in MFP and dorsal neural cells, respectively. (**A-F**) Expression of *nkx2.9* (A,D), *arx* (B,E) and *pax7a* (C,F) on transverse sections of ctrlMO- (A-C) and *sulf1*MO- (D-F) injected embryos at 24hpf. Asterisks in all panels mark MFP. Scale bar=20µm.

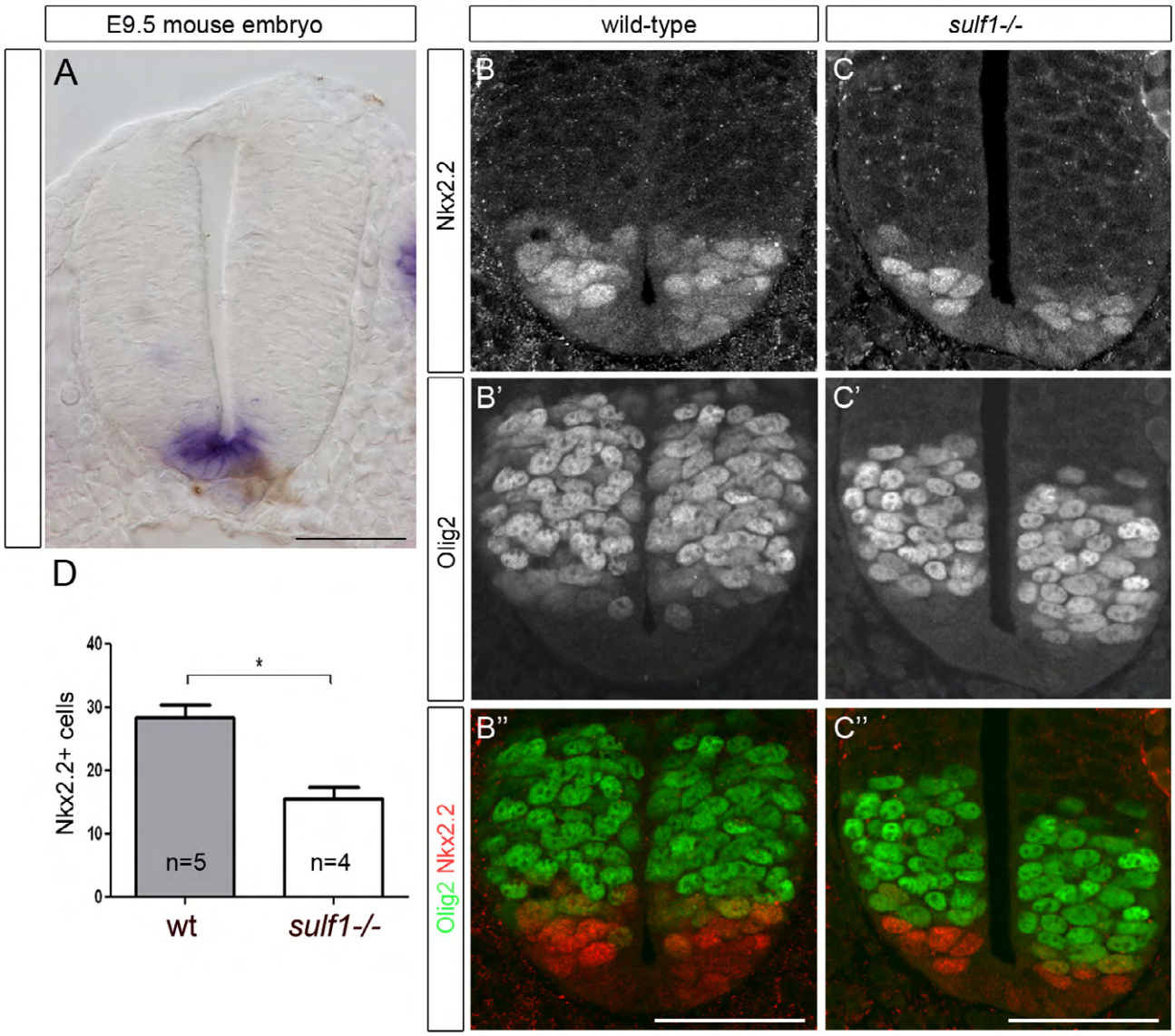

Figure S4. Sulf1 depletion impairs formation of the p3 domain in mouse. All panels show transverse section of E9.5 mouse spinal cord at mid-gut level. (A) Detection of *sulf1* mRNA. (B-C") Double detection of Nkx2.2 (B,C red in B" and C") and Olig2 (B'-C', green in B"-C") in wild-type (B-B") and *sulf1* mutant (C-C") mouse embryos. Note that dorsal extension of the Nkx2.2+ domain is reduced in *sulf1* mutant embryos (compare B and C). (D) Quantification of Nkx2.2+ cells in wild-type (Wt) and *sulf1* mutant (*sulf1-/-*) embryos. Results are expressed as mean number of cells±s.e.m. (*p<0.02). Scale bars = 100 µm in all micrographs.

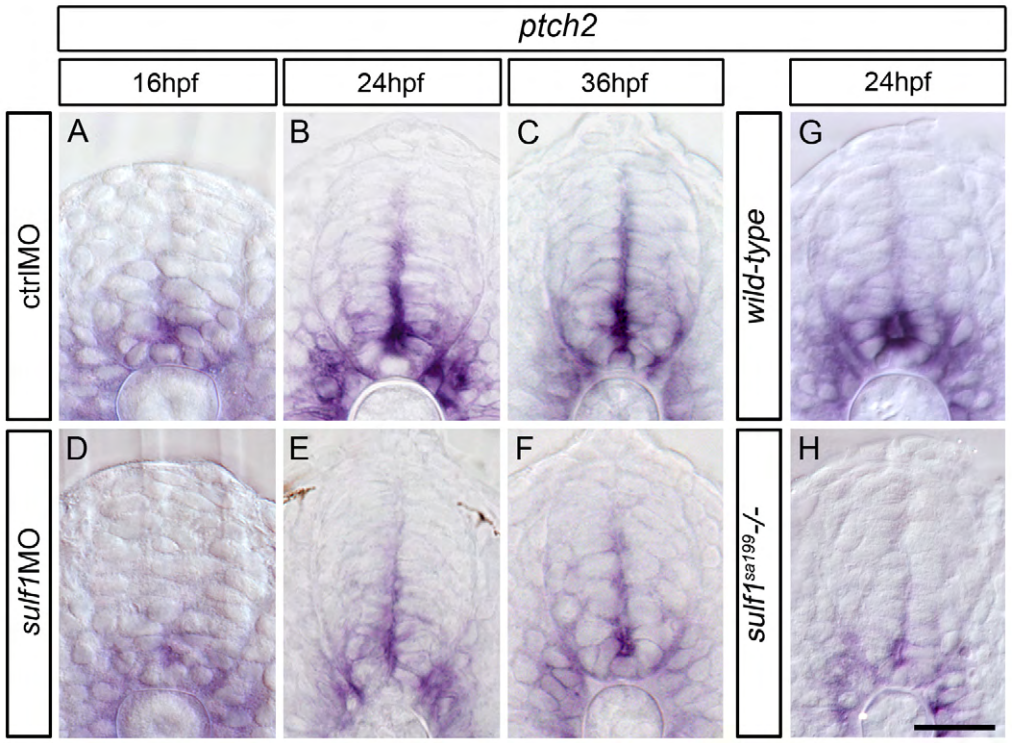

Figure S5. Shh signaling activity is reduced in *sulf1*-depleted zebrafish embryos. (A-F) Expression of *ptch2* at 16hpf (A,D), 24hpf (B,E) and 36hpf (C,F) in embryos injected with ctrlMO (A-C) and *sulf1*MO (D-F). (**G,H**) Expression of *ptch2* at 24hpf in wild-type (G) and *sulf1*^{sa199}-/- (H) embryos. Note reduction in *ptch2* expression both in *sulf1*MO-injected and *sulf1*^{sa199}-/- embryos at 24hpf. Scale bar = 20μm.